Authors' responses to reviewer comments

"Inverse modeling of fire emissions constrained by smoke plume transport using HYSPLIT dispersion model and geostationary observations"

General response

Authors express their appreciation to the two reviewers and the editor. Thanks to their productive comments, we were able to improve our manuscript. As the reviewer recommended, we have included additional tests and discussions on the sensitivity. Mistakes were revised, and performance statistics were also updated. We provide below the general responses and the point-by-point responses to the reviewer's comments. Reviewers' comments are shown in italics.

Here are three major points in the revised version of the manuscript.

1. Sensitivity tests for temporal coverage

As both reviewers commented, we agree that the temporal sensitivity section needs a clarification of the goal. Our original intention was to find the most efficient temporal coverage of the inverse system to conduct the assimilation process, which includes both time windows for the assimilation and the use of observational data. On the other hand, the reviewers asked to test the sensitivity by the change of observational data use. We believe that both tests are meaningful, so we included both test results in the manuscript. The former is important in terms of the efficiency of the inverse system because dispersion simulations to construct the TCM is the most time-consuming processes in the inverse system. The latter, selection of observations (used in the assimilation), is also important to investigate the responses of the inverse system.

Indeed, there are three adjustable time windows in the processes and evaluation of fire emission assimilation. As shown in **Figure R1**, the assimilation (or analysis) time window denotes the temporal coverage of fire emission sources and simulated dispersions. The observational data time window (or selection of observations used for constraining in the assimilation) can be set equal to or shorter than the assimilation time window. The evaluation time window (or selection of observations used for evaluation) is also set equal to or shorter than the observational time window. Therefore, we tested combinations of these time windows.

1) Assimilation time window (source, dispersion and assimilation process)
2) Observation time window (observation)
3) Evaluation time window (model and observation)

Model performance statistics were calculated with combinations of temporal coverages of assimilation (shown as "A" in Table R1; 24h-96h), observation (shown as "O", 24h-96h), and evaluation (shown as "E", 24h-96h). Results are summarized in Table R1. As discussed in the manuscript, including more analytical period generally improves the performance of the inverse system, but the difference is not critical for more than 48-hour time window.

With fixed analytical period (A:96h), performance statistics are better with shorter observational time window applied. It makes sense because we expect to have a better fit with smaller number of data points during the analysis process although it also has a risk of potential overfitting problem, as the reviewer #2 commented.

The manuscript was revised to include these additional sensitivity tests.

(Line 270) "First, we changed the assimilation time windows from one (24-hours) to four days (96-hours). Since the impact of fire emissions easily translates over multiple days, we tested how temporal coverage affects system results. The 'one-day' (aday=0) simulation is run through the inverse model using dispersions and observations for the target day, while the 'two-day' simulation uses two days (i.e., 48 hours) of dispersions and observations (aday=-1). For this test, all observations within the

assimilation time windows were selected for the assimilation and the evaluation. The results are shown in **Figure 6a**, while the correlation and error statistics are summarized in the top section of **Table 2** (i.e. [A:24h, O:24h, E:24h], … , [A:96h, O:96h, E:96h]). With the exception of November 10 and 11, in the early stage of the fire event, both the correlation coefficient (R) and normalized root-mean-square error (NRMSE) were improved by the use of more days (i.e., three or four days) of dispersions and observations for the inverse model. This makes sense, because emissions from multi-day fire events spread out and affect concentrations over proceeding days.

A series of additional simulations were also conducted to test the system's sensitivity to the selection of observations for the assimilation and the evaluation. In these tests, we investigated combinations in assimilation time ("A" in **Table 2**), observational time ("O") and evaluation time windows ("E"). Results are also summarized in **Table 2**. For a fixed assimilation time period (i.e. [A:96h]), using shorter observational time window resulted in a better result. It is reasonable because we expect a better fitting with smaller number of data points. However, it can be easily exposed to overfitting problem if available data for the assimilation is too small."

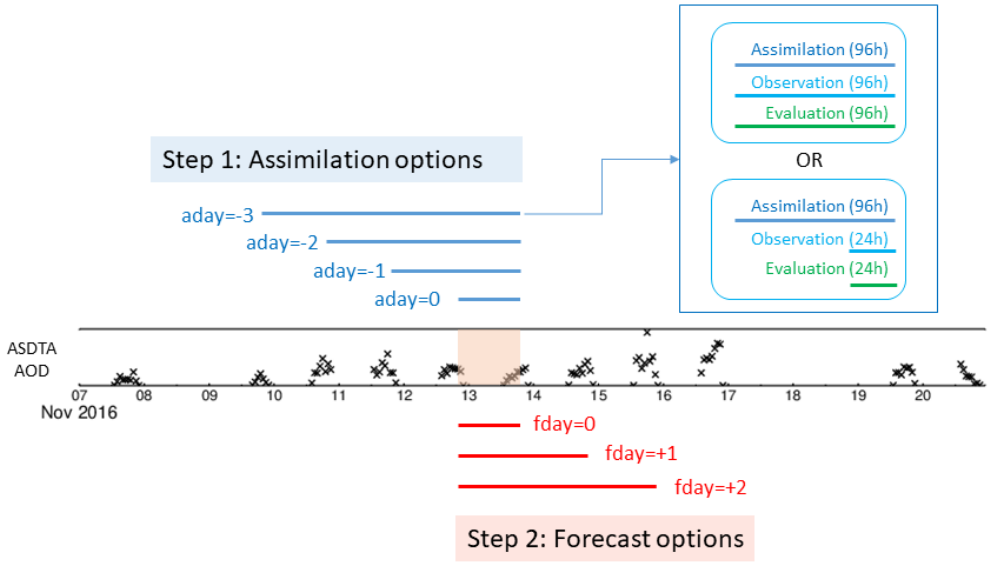

Figure R1 Two steps for smoke forecast with the HEIMS-fire system. Temporal coverage of assimilation days (aday=0,-1, -2,-3) and forecast days (fday=0,+1,+2) for operational tests. Assimilation process includes three time windows – assimilation, observation and evaluation time windows.

Table R1 Sensitivity test for temporal coverage. Uses of analysis (A), observation (O), and evaluation (E) time windows (24 hours to 96 hours) were tested, and statistics, NRMSE and R, were compared. The best performance is marked as bold.

	NRMSE (%)				R			
Coverage	A: 24h O: 24h E: 24h	A: 48h O: 48h E: 48h	A: 72h O: 72h E: 72h	A: 96h O: 96h E: 96h	A: 24h O: 24h E: 24h	A: 48h O: 48h E: 48h	A: 72h O: 72h E: 72h	A: 96h O: 96h E: 96h
Nov. 10	66.6	63.7	**62.7**	68.7	**0.677**	0.654	0.669	0.577
11	75.2	65.9	64.0	**63.7**	0.410	**0.620**	0.587	0.593
12	75.1	63.5	61.4	**60.6**	0.373	0.309	**0.562**	0.526
13	72.8	65.7	59.9	**59.6**	0.298	0.476	0.397	**0.576**
14	75.6	66.3	61.0	**56.8**	0.285	0.444	**0.522**	0.469
15	82.7	70.9	62.7	**60.2**	0.105	0.348	0.465	**0.511**
16	69.8	72.5	68.2	**61.7**	0.146	0.150	0.372	**0.478**
17		69.8	72.5	**68.2**		0.146	0.150	**0.372**
Coverage	A: 24h O: 24h E: 24h	A: 48h O: 48h E: 24h	A: 72h O: 72h E: 24h	A: 96h O: 96h E: 24h	A: 24h O: 24h E: 24h	A: 48h O: 48h E: 24h	A: 72h O: 72h E: 24h	A: 96h O: 96h E: 24h
Nov. 10	66.6	49.1	49.0	**38.7**	0.677	0.713	0.716	**0.716**
11	75.2	80.6	78.4	**78.4**	0.410	0.621	0.623	**0.623**
12	75.1	**45.2**	56.5	55.8	0.373	0.406	0.425	**0.430**
13	72.8	58.0	**52.9**	63.5	0.298	0.534	0.581	**0.589**
14	75.6	54.6	53.8	**53.1**	0.285	0.567	0.593	**0.609**
15	82.7	43.9	**42.4**	44.6	0.105	0.554	**0.589**	0.571
16	69.8	34.3	28.4	**27.4**	0.146	0.464	**0.507**	0.505
17								
Coverage	A: 96h O: 24h E: 24h	A: 96h O: 48h E: 48h	A: 96h O: 72h E: 72h	A: 96h O: 96h E: 96h	A: 96h O: 24h E: 24h	A: 96h O: 48h E: 48h	A: 96h O: 72h E: 72h	A: 96h O: 96h E: 96h
Nov. 10	**53.0**	62.1	62.1	68.7	**0.746**	0.657	0.657	0.577
11	**54.7**	61.9	63.7	63.7	0.583	**0.615**	0.593	0.593
12	**43.0**	54.0	59.1	60.6	0.425	0.481	**0.545**	0.526
13	**40.3**	46.4	54.5	59.6	**0.664**	0.510	0.500	0.576
14	**38.3**	43.5	50.5	56.8	**0.688**	0.603	0.499	0.469
15	**43.9**	50.8	55.3	60.2	**0.647**	0.572	0.533	0.511
16	**33.5**	42.2	53.2	61.7 68.2	0.667	**0.685**	0.581	0.478
17		36.1	53.8			**0.624**	0.520	0.372
Coverage	A: 96h O: 24h E: 24h	A: 96h O: 48h E: 24h	A: 96h O: 72h E: 24h	A: 96h O: 96h E: 24h	A: 96h O: 24h E: 24h	A: 96h O: 48h E: 24h	A: 96h O: 72h E: 24h	A: 96h O: 96h E: 24h
Nov. 10	53.6	47.1	47.1	**38.7**	**0.746**	0.715	0.715	0.716
11	**58.1**	81.0	78.4	78.4	**0.668**	0.624	0.623	0.623
12	**41.3**	48.0	56.7	55.8	**0.489**	0.432	0.433	0.430
13	**39.5**	49.8	55.4	63.5	**0.691**	0.612	0.588	0.589
14	**39.5**	45.8	51.9	53.1	**0.698**	0.612	0.612	0.609
15	**37.8**	43.1	43.1	44.6	**0.682**	0.552	0.566	0.571
16	**33.7**	29.6	27.9	27.4	**0.614**	0.542	0.510	0.505
17								

2. Sensitivity tests for vertical layer selection

For the sensitivity of vertical layer configuration, we added an extra test as the reviewer #2 suggested. With the maximum height fixed at 5,000m, we conducted a sensitivity test by increasing vertical layer resolution from 2 layers to 6 layers. As expected, we have better performance statistics as we increase the number of layers although the change is not dramatic after four layers (**Table R2**).

Indeed, this vertical layer sensitivity is one of the most important topics in the construction of smoke forecast system since it is directly related to the smoke plume rise problem. Therefore, we believe that the topic deserves a separate effort. We are preparing a follow-up study on the plume rise options, based on plume rise parameterization (in HYSPLIT) and inverse modeling technique. For current study, we like to narrow and focus on its own scope. While we demonstrate vertical layer selection sensitivity from its maximum height and vertical layer resolution, detailed analysis on the fire emission plume rise options warrants an additional full research.

Table R2 Sensitivity tests for vertical layers resolution from two to six layers. The best performance is marked as bold.

	Date	2 layers (100, 5000m)	3 layers (100, 2000, 5000m)	4 layers (100, 1000, 2000, 5000m)	5 layers (100, 1000, 1500, 2000, 5000m)	6 layers (100, 500, 1000, 1500, 2000, 5000m)
NRMSE	Nov. 10	72.9	69.2	65.9	63.7	**63.7**
	11	79.0	71.6	68.1	66.4	**65.9**
	12	70.7	67.8	65.5	65.0	**63.5**
	13	68.7	67.6	66.1	65.9	**65.7**
	14	72.9	70.6	67.2	67.0	**66.3**
	15	83.3	77.1	72.0	71.0	**70.9**
	16	78.9	**72.0**	73.2	72.5	72.5
	17	72.2	70.6	70.2	70.0	**69.8**
R	Nov. 10	0.577	0.593	0.630	0.654	**0.654**
	11	0.490	0.558	0.598	0.614	**0.620**
	12	0.292	0.285	0.303	0.303	**0.309**
	13	0.449	0.450	0.468	0.470	**0.476**
	14	0.404	0.419	0.439	0.440	0.444
	15	0.252	0.276	0.338	0.346	**0.348**
	16	0.112	**0.164**	0.144	0.149	0.150
	17	**0.198**	0.139	0.139	0.139	0.146

The manuscript was revised including this information.

(Line 286) “Second, we tested the layers at which fire emissions are initiated in the model. As expected, including more layers results in better statistics, since the transport and dispersion of each smoke plume can vary with the altitude to which their fire emissions are allocated. We tested the model’s uncertainties on layers’ maximum extension and resolution, with varying selections of two to seven layers at 100, 500, 1000, 1500, 2000, 5000, or 10000 meters. To test the maximum extension, starting from two layers (i.e. with emissions released at 100 and 500 meters), we added the next higher layer over six test runs to investigate the effect of maximum extension of smoke plume. **Figure 6b** shows the results, and error statistics are summarized in **Table 3.** Including the 5000m layer, especially, resulted in noticeable changes, implying the potential benefit of including high-level transport for specific days. Since the 5000m layer is above typical planetary boundary layer height, emissions injected at this level experience different physical characteristics. Smoke lofted into the free troposphere is less affected by turbulence and scavenging, and transports easily hundreds or thousands of kilometers downwind because of the higher wind speeds. Addition of the 5000m layer would better represent the potential long-range transport. Smoke plume rise is one of traditionally important questions in smoke modelling, so further research on the topic is warranted. Effects of the layer resolution were also tested. Starting from two layers (i.e. 100m and 5000m), we added intermediate layers up to six layers, and evaluated their performances (**Table S3**). As expected, including more layers resulted in the better statistics, but its improvement was not significant after four layers. “

3. Scope of the study

Here, we like to address the scope of this manuscript again. In this study, we intended to conduct two goals: 1) Suggestion of inverse modeling framework, and 2) improvement of operational smoke forecasts. Our main priority here is to suggest a practical framework to help fire emission estimation. However, for the second goal, we do not claim that our new system is a complete solution and outperforms in all aspects because we know that many uncertainties remained to be resolved until we claim a clearly better forecast system. To improve the forecasting system, we admit that we need more improvement in other components, including the quality of satellite products (to monitor the dispersion of smoke plume), better meteorology and fire activity persistency, as we discussed in the manuscript.

We also provide point-by-point responses to each reviewer.

REVIEWER #1

- In section 1 (Introduction), there is no background information of applications of inverse modeling on fire emissions estimations. As this is the focus of this work, it would be helpful to inform readers about previous investigations on this topic, as well as to highlight the features and advantages of the inverse modeling system proposed in this work.

Thanks for the comment. We included some of previous inverse modeling efforts, but its application to fire emission estimation is limited. Most of fire emission estimations use a survey-based bottom-up or a satellite-based top-down approaches by simple comparison. While we agree that those efforts are valuable, we see that the inverse modeling technique is rarely used, especially for using smoke transport as a constraint. We included this information in the manuscript.

(Line 82) "Such an approach has been adapted to estimate inversely various emission sources, including greenhouse gas emissions (Kunik et al., 2019; Nickless et al., 2018; Turnbull et al., 2019), volcanic ashes and sulfur dioxide emissions (Boichu et al., 2014; Crawford et al., 2016; Zidikheri and Lucas, 2020), and radionuclide release from nuclear power plant incident (Chai et al., 2015; Katata et al., 2015; Li et al., 2019a), but was rarely used in fire emission estimation (e.g. Nikonovas et al., 2017)."

- The HYSPLIT model used to compute dispersion factors using the TCM approach is described in section 2.3, but some details are not provided, e.g., the temporal resolution of the HYSPLIT integration and the TCM results. Also, deposition considered by using a radioactive decay constant. Is it equivalent to the deposition process of fire smoke aerosols? How does it compare with the deposition considered in other Eulerian air quality models with more comprehensive chemistry?

Thanks for the comment. We included additional information of HYSPLIT configuration and output specification. For each day's inverse process, we saved HYSPLIT simulation outputs hourly, and ASDTA AOD were also produced hourly. The integration time step of HYSPLIT cannot be specified because it can vary during the simulation, being computed from the requirement that the advection distance per time-step should be less than the grid spacing. The maximum transport velocity is determined from the maximum transport speed during the previous hour. HYSPLIT handles dry and wet deposition of particles. Smoke particles are subject to dry deposition (including turbulent diffusion) in addition to gravitational settling and wet removal using meteorological model precipitation. Similar to other chemistry models, wet removal is defined as a scavenging coefficient to handle below- and within-cloud processes, although their parameterization would be model-specific. Please, see Stein et al. (2015) for detailed information of HYSPLIT procedures. Manuscript was revised to address the consistency to the previous system.

Radioactive decay is used for nuclear dispersion study. It is irrelevant for the study, so was removed.

(Line 130) "Hourly outputs were integrated to match with satellite observational data. HYSPLIT modelling options were configured to be consistent with the SFS system, including options for dry and wet depositions (i.e. 0.8 μm diameter with 2 g/cm^3 density) (Rolph et al., 2009).

- In the HYSPLIT simulations, dispersed concentrations were vertically integrated up to 5000 m to get partial column mass loading of smoke particles. Is there any reference for the selection of the column height (5000 m)? In addition, smoke loading from satellite observations is converted from AOD using a constant conversion factor. Could the authors further discuss the possible uncertainties that could be introduced by using this constant conversion factor? For example, how is this constant conversion factor compare with values reported by previous literature, and is there any relation between the conversion factor and other plume features (e.g., plume age)? And, this uncertainty can be considered in observation errors in the inverse modeling system.

Thanks for the comment. Most of HYSPLIT modeling settings in this study are configured to be consistent with the current operational system as described in Rolph et al. (2009).

With current design, the inverse system generates the best fit for given situation. Selection of conversion factor does affect the absolute values of both model and observation, but does not affect

their relative comparison (e.g. NRMSE, R). We have tested different conversion factors, and results are consistent in terms of their variations regardless of conversion factor assumption. However, it-should be noted that application of dynamic conversion factor (e.g. conversion factors varying depending on location and time) may affect the output, so better treatment of conversion factor will be required for more realistic inverse modeling process in the future. In current system, we include the observational error of AOD, but does not include error term from the conversion factor. We have included this information in the manuscript.

(L135) "Although we used a single conversion factor for the study, the actual conversion factors may vary in time and space (i.e. 3.9 – 5.3 m^2/g) (Chand et al., 2006; Hobbs et al., 1996; Ichoku and Ellison, 2014; Nikonovas et al., 2017; Reid et al., 2005). Therefore, applying more realistic conversion factors and their uncertainties into the system would be another factor in the future improvement of the system."

- In section 3.2 of the cost function used in the inverse system, the estimations of error have not been provided, which are important terms for the inversion method. Firstly, how are the background error variances evaluated, and how does the value used here compare with typical uncertainties of fire emissions? Secondly, as mentioned in section 2, the observation error variances are composed of uncertainties in Lagrangian model, observations, as well as representative errors. It would be important to include more details about the determination of these error components. Thirdly, what kind of error terms should be considered in F_{other} and how are they determined?

Thanks for the comment. The manuscript has been modified to provide the estimations of error terms used in the cost function. The added text is shown below to address these issues. In addition, three references are added as well.

(Line 168) "A background term is included to measure the deviation of the emission estimate from its first guess, q_{ikt}^b, obtained from the operational BlueSky emission computation. The background term ensures the problem remains well-posed even with the limited observations available in certain circumstances. The background error variance σ_{ikt}^2 measures uncertainties in q_{ikt}^b. Pan et al. (2020) compared six global emission estimates and found that the total emission differs by a factor of 3.8. However, emission estimations at specific locations and times can have much larger errors. In addition, the vertical distribution of the smoke emissions is difficult to determine and this adds even more uncertainties to the emission estimates. We chose a large uncertainty for the background term as $\sigma_{ikt\_}=1000\times q^{b}_{ikt}+ 1000$ kg/hr at all locations and heights to minimize the adverse impact of inaccurate BlueSky emission estimates. The observational error variances, ε_{nm}^2, represent uncertainties in both the model and observations, as well as the representative errors. Kondragunta et al. (2008) indicated that GOES aerosol retrievals over land were expected to have uncertainties within $0.15\tau \pm 0.05$, where τ is the AOD. Paciorek et al. (2008) showed a better performance of GOES aerosol retrievals in eastern U.S. than in western U.S. Green et al. (2009) demonstrated that GOES AOD correlates best with AERONET in autumn (September to November) than in other seasons. They showed that the RMS error was 0.060 in autumn while the average for all seasons is 0.0149. Considering the better performance in the Eastern US and in November, AOD uncertainties of $0.10\tau \pm 0.06$ are assumed in this paper. A slightly larger additive component of the AOD error is chosen to include the effects of the representative errors and model errors which do not vary with the observed AOD values. F_{other} refers to the other regularized terms that can be included in the cost function. For instance, Chai et al. (2015) has a temporal smoothness penalty term to avoid abrupt changes in the temporal profile of the release rates. While this optimization problem could be solved to obtain optimal emission estimates using many minimization tools, we used the Limited-Memory Broyden–Fletcher–Goldfarb–Shanno (BFGS) algorithm (Zhu et al., 1997)."

Christopher J. Paciorek, Yang Liu, Hortensia Moreno-Macias, and Shobha Kondragunta: Spatiotemporal Associations between GOES Aerosol Optical Depth Retrievals and Ground-Level PM2.5, Environmental Science & Technology 2008 42 (15), 5800-5806, DOI: 10.1021/es703181j

Green M, Kondragunta S, Ciren P, Xu C. Comparison of GOES and MODIS aerosol optical depth (AOD) to aerosol robotic network (AERONET) AOD and IMPROVE PM2.5 mass at Bondville, Illinois. J Air Waste Manag Assoc. 2009;59(9):1082-1091. doi:10.3155/1047-3289.59.9.1082

Pan, X., Ichoku, C., Chin, M., Bian, H., Darmenov, A., Colarco, P., Ellison, L., Kucsera, T., da Silva, A., Wang, J., Oda, T., and Cui, G.: Six global biomass burning emission datasets: intercomparison and application in one global aerosol model, Atmos. Chem. Phys., 20, 969–994, https://doi.org/10.5194/acp-20-969-2020, 2020.

- The ASDTA smoke AOD data are assimilated in the HEIMS-fire system to obtain inverse estimation of fire emissions. As indicated in the introduction, the ASDTA data are based on automatic detections of fire smoke plume and represent smoke AOD, which means that the background AOD has been subtracted from total value. Is it correct? Then could the authors explain how is the background AOD derived? Also, the uncertainties in background AODs can impact inversion results, because an overestimation of background AOD will lead to underestimated smoke AOD (then underestimated fire emissions) and vice versa. This uncertainty can also be considered in the observation errors used for inversion.

Thanks for the comment. The ASDTA smoke AOD is not determined by subtracting the background AOD from the total AOD. The radiative signatures of an aerosol layer are determined by the scattering and absorption properties of the aerosol within a layer in the atmosphere. Reflectance value of the 0.86 μm channel (R0.86μm) divided by the reflectance value of the 0.63μm channel (R0.63μm) is often used to determine the aerosol type. Presence of smaller aerosols, like smoke, tends to reduce the values for this ratio, as smaller particles are more efficient at scattering light at 0.63μm. In addition, ASDTA also utilizes a pattern recognition technique to isolate smoke aerosols from other type of aerosols. The background AOD is not directly used to retrieve ASDTA smoke AOD. We utilize the observational error information of ASDTA AOD in the inverse modeling system.

(Line 111) “For each pixel, the radiative signatures of an aerosol layer (e.g. dust and smoke) are determined by the scattering and absorption properties of the aerosol. ASDTA also utilizes a pattern-recognition technique to isolate smoke aerosols from other type of aerosols, so it can recognize plumes transported far from fire sources.”

- In section 3.3, the naming conventions of inversion and forecasting processes are described. It’s a bit inaccurate to say that “fire emissions on November 13 can be estimated using ASDTA observations for 24 hours (i.e. oday=0), 48 hours (i.e. oday=-1), 72 hours (i.e. oday=-2), and 96 hours (i.e. oday=-3).” Technically, if we focus on fires on the target day (oday = 0), the regional impact and transported smoke plumes from those fires would be found on the following days (oday=1, 2, 3, etc.). Therefore, in this case the emissions on November 13 can only be constrained by the observations on oday=0 in reanalysis mode. On the other hand, the observations on oday=0 can constrain emissions on oday=0, as well as emissions on previous days simultaneously. So, the major benefit of including more observational days is getting more constraints for fires on multiple days, and providing a better estimation of the background smoke plume for the target day. In this case, it would be more precise to say that “for a target day of November 13, inversions are conducted using ASDTA observations for 24 hours (i.e. oday=0), 48 hours (i.e. oday=-1), 72 hours (i.e. oday=-2), and 96 hours (i.e. oday=-3).”

Thanks for the comment. Descriptions on the analytical and observational time windows are revised. Also, see discussions in the general response #1.

(Line 207) “This inverse system is designed to estimates fire emissions on the target day by analyzing past and present smoke field, and then utilizes them to forecast the future smoke field. The assimilation days (i.e. aday = 0,-1,-2) (see **Figure S1**) indicate the temporal coverage of dispersions and constraining observations. For a target day of November 13, inversions are conducted using HYSPLIT dispersion simulations and ASDTA observations for 24 hours (i.e. aday=0), 48 hours (i.e. aday=-1), 72 hours (i.e. aday=-2), and 96 hours (i.e. aday=-3). Estimated fire emissions are used to

simulate fire smoke for November 13 (i.e. fday=0; reanalysis), and the same amount of fire emissions are used in forecast mode for November 14 (i.e. fday=+1) and 15 (i.e. fday=+2). "

- Column particle mass loading is used to constrain fire smoke emissions, and emissions released at different numbers of vertical layers are tested in the sensitivity analysis. Including 5000 m level make an obvious improvement for the results. But there is a lack of analysis for the reason. A possible reason is that, 5000 m is usually above the Planetary Boundary Layer Height (PBLH). So, it would be interesting to examine the PBLH and plume injection height for this case, since smoke injection height is important to smoke transport. Smoke lofted into the free troposphere is often transported hundreds or thousands of kilometers downwind because of the higher wind speeds, generally lower turbulence levels, and less scavenging processes at higher altitudes. While, smoke trapped within the PBL is usually well mixed, and remains near the source region. If most of the fire spots in this case showed injected emissions above the PBLH, then it means that, including 5000 m in the simulations allows a better representation of emission injection, and the plume can be transported further and better constrained by observations.

Thanks for the comment. We agree with the reviewer's comment. We included discussions on the vertical layer extension. Also, see the general response #2.

(Line 292) "Including the 5000m layer, especially, resulted in noticeable changes, implying the potential benefit of including high-level transport for specific days. Since the 5000m layer is above typical planetary boundary layer height, emissions injected at this level experience different physical characteristics. Smoke lofted into the free troposphere is less affected by turbulence and scavenging, and transports easily hundreds or thousands of kilometers downwind because of the higher wind speeds. Addition of the 5000m layer would better represent the potential long-range transport."

- As a follow-up of the last comment, could it provide better results by tuning the emission release heights incorporating information from a plume rise model?

Thanks for the comment. We agree that plume rise models can help by providing 1) better initial guess of vertical allocation of emissions, and 2) complementary simulation when observations are limited. Please, also see the general response #2.

- For the sensitivity test on the time range of observation data used in inversion, "The 'one-day' (oday=0) simulation is run through the inverse model using dispersion and observations for the target day, while the 'two-day' simulation uses two days (i.e., 48 hours) of dispersion and observations (oday=-1)". As this sensitivity test focus on the time range of observations, I think it is unfair to compare the results using different days for both of dispersion and observations. For example, if we compare the results using 'one day' and 'two days' shown in the current test, for the 'one-day' simulation, all the mismatches of modeled and observed smoke mass loading would be attributed to adjustments of fires on the target day, which would likely lead to a significant error in the emission estimates for the target day. While the 'two-day' simulation allows the fires on oday=-1 to be constrained at the same time. Therefore, it would make more sense to use four days of dispersion for all the simulations for this test, and just change the observation days from 1 (24 hours) to 4 (96 hours).

Thanks for the comment. We clarified the temporal coverage sensitivity test. Please, see the general response #2.

- At the end of section 4.3, it is mentioned that "The November 17 output shows how the system responds when observations are limited or missing, although it still provides a robust result by honoring the initial guess information". But no result is referred. It would be clearer to add a reference to the figure/table supporting this sentence. If it is Figure 4, it would also be better to indicate the number of points in each panel to show that the observations are limited on Nov 17, given that many points could be overlapped.

Thanks for the comment. Although November 17 has no ASDTA AOD, the inverse system still produced a reasonable output (Figure 5). We included discussion on the performance of the inverse system with limited observational data.

(Line 25) "The November 17 output in **Figure 5** shows how the system responds when observations are limited or missing, although it still provides a robust result by honoring the initial guess information. On November 17, no ASDTA AOD was provided from the satellite operation. Under 48-hour configuration (i.e. aday=-1), the inverse system still produced reasonable outputs using limited observations (November 16) and initial guess emissions (November 16 and 17)."

- P8, L249-255, this paragraph can be more concise. Also, a description of the result of the spatial coverage sensitivity test is missing.

Thanks for the comment. We removed unnecessary sentences. We also included discussions on the spatial coverage sensitivity test result.

(Line 301) "In the third test, we varied the spatial coverage of input fire information. Although wildfire impacts easily spread by long-range transport, we could not include all the global fire information due to limited computational resources. We therefore tested different spatial domains of fire locations to evaluate what spatial coverage of wildfire detection information is required to estimate fire emissions. Fire sources inside domain 1 through 4 (**Figure 3**) were tested in the assimilation constrained by ASDTA AOD inside Domain 1. **Figure 6c** and **Table 4** show correlation and error statistics from the sensitivity test of spatial coverage. In most days, we have better results when we include fire emission sources at least within domain 2. It makes sense considering the effects of transported fire plumes form Mississippi and Louisiana (**Figure 3**). Maximizing geographical coverage (e.g. domain 4) did not always result in the best performance in our case study. This result, however, should be taken carefully because we do not have strong fire activities outside domain 2 in our study case. Strong long-range transport cases, typically form northwestern US, Canada and Alaska, would have bigger impacts. "

- As stated in section 4.5, for the forecasting days, smoke is estimated as the summation of impact from fires existed on previous days and new emissions on the target days, and fire plumes initialized on fday =0, 1, 2 are used here for the summation. How do the authors determine how many previous days should be considered? Since the impact of fires can extend to multiple days, would it give a better result by adding the contribution of smokes initiated on the analysis days, e.g. oday = -1, -2, and -3?

Thanks for the comment. This is a key point of the temporal coverage sensitivity tests. Theoretically, we expect better output when we use longer temporal coverage, but it requires more computational resources. Current sensitivity test suggests that 48-hour time window can provide a decent result. In a forecast mode, we see the effect of persistency rate seems to be larger than other factors. Therefore, in the actual application of forecast system, more tuning of the system is required.

- In the abstract, it is concluded that the inverse modeling system developed here outperform than the current operational forecast product in terms of RMSE, but it's not clear RMSE of which variable is denoted here, and what observation dataset are the hindcast results and operational product evaluated against.

Thanks for the comment. Evaluations were conducted for smoke mass loading between hindcast and operational product against satellite-observed fire smoke mass loading for next 48-hour.

- P3, L92: "A modeling framework" -> "As a modeling framework"

Corrected.

- P4, L95: emission rate or emission? Do they represent the same term in this paper (i.e. fire smoke particles emission)? It seems that both are used throughout this paper. It would be better to use one of them and keep consistent.

Thanks for the comment. Conceptually, it is ‘emission’ in general, and ‘emission rate’ is used as an actual input for the HYSPLIT. We used ‘emission rate’ specifically for cost function minimization or as a model input.

- P4, L125: I do not quite understand why “the results shown in the study are obtained by multiplying the column height (i.e. 5000 m)” here. It has been shown that, the column TCM is calculated by integrating dispersed concentrations vertically, so the TCM is already in units of column loading per unit emission. Is it correct?

Simulation outputs for TCM are in density unit and are converted to column mass loading by multiplying column height.

- P7, L189: true color image. There is not a true color channel.

Corrected.

- P7, L214: “estimation of assimilated fire emissions” -> “estimation of fire emissions”

Corrected.

- Section 4.3, the time range of observations assimilated in this case experiment is not indicated.

As mentioned in captions of Figure 4 & 5, 48-hour observations are used.

- What’s the date for the result shown in Figure 5?

Dates are labeled in the left side of each panel. We specified the period in the caption.

- P8, L225: remove “that”

Revised.

- P8, L242: “smoke dispersions” -> “fire emissions”

Corrected.

- P8, L247, “As expected, including more layers generally produce better result.” This sentence is nearly a duplication of the sentence in L242-243.

Thanks for the comment. We removed the sentence.

- P10, L295: “From the top panel of Figure 9” -> “For the top panels of Figure 9”

Corrected.

- P10, L295: “are solely originated fires” -> “are solely originated from fires”

Corrected.

- P10, L303: “reply on” -> “rely on”

Corrected.

- P10, L312, for the “additional constraint”, “transported smoke plume” could be better. There are other places of this term, please consider revising them accordingly.

Thanks for the comment. We revised sentences.

REVIEWER #2

1. How the experiments with different assimilation time windows are run needs to be made clearer. Is it the case that in all experiments the emissions are initiated at the same locations and times, the only difference being the satellite data assimilation time window? If that is the case, can you clarify why longer time windows results in better agreement with observations for the analysis? I would have thought it would be easier to fit the model to data from one timestep than to fit the model to data from different timesteps. I can not quite understand the explanation given in the paper (e.g. Line 240), which I interpret to mean that this is due to emissions at (x1,t1) affecting the smoke field at (x2,t2). This is true, but I would expect better results for the smoke field at (x2,t2) if there was no observation at (x1,t1) because the emission at (x1,t1) would only be constrained by the observation at (x2,t2) and not (x1,t1) and (x2,t2) simultaneously. You probably also need to clarify which data points are included in the verification statistics (for example, when you assimilate data on day 0, do you calculate verification statistics based on day 0 only or do you also include days -1, 2 etc?).

Thanks for the comment. We agree that the temporal coverage sensitivity section needs improvement. Please, see the general response #1.

2. In performing the forecasts, it is not completely clear whether you are using NWP analysis data to drive the forecasts, or you are using NWP forecast data. If this system is to be used operationally, then clearly NWP forecasts will need to be used, which we expect will result in poorer forecasts than when the NWP analyses are used. I think this needs to be clarified.

Thanks for the comment. This is a fair comment. At this point, we don't have an archive of full length of everyday NAM forecast, so our hindcast has an advantage over operational runs in terms of meteorology. We revised the manuscript to address it.

(Line 316) "Notable differences in the configuration of SFS and HEIMS are plume rise estimation, temporal resolution of fire emissions, fire decaying assumption, and meteorology. While SFS computes plume rise using the Briggs' equation (Arya, 1998; Briggs, 1969), which assumes an air parcel's rise is based only on the buoyance terms, HEIMS determines fire emissions' vertical allocation using an inverse system. At the initial guess, SFS fire emissions are evenly distributed in all layers. Current HEIMS assumes daily emission variation compared to hourly emissions of SFS. Also, SFS assumes 75% of emissions still happen at the same location the next day, the HEIMS uses 50% decay assumption after sensitivity tests, which will be discussed in the next section. For HEIMS simulation, we used aday=-1 (two-day temporal coverage) for the simulations shown. On the other hand, HEIMS would be benefitted with a better meteorology. Although both systems use the NAM12 forecast meteorology, HEIMS hindcast used the first 24 hours portion of everyday forecast cycle, and SFS used 72 hours forecast."

3. Nothing has been said about analysis and forecast errors. Can this system be used to predict errors (uncertainty) or is it purely deterministic? I think some comments on this issue in the paper would be useful.

Thanks for the comment. Uncertainties in the analysis processes include the quality of inputs (i.e. observations, dispersion, and meteorology). Although the system is not purely deterministic, it is difficult to estimate the uncertainties of the results without knowing the meteorological input errors. Performing an ensemble of HYSPLIT predictions using different meteorological inputs can provide some insight in this respect. We added the following text to the conclusion.

(Line 382) "It also should be noted that the uncertainties of the emission estimation and the smoke forecasts thereafter are not quantified in this study. An ensemble of HYSPLIT predictions using different meteorological inputs will be used to estimate the uncertainties of the results in the future."

1. In the abstract you have several acronyms that are only defined later in the text. These must be defined in the abstract or alternatively think about removing them altogether from the abstract. In my view they are not that important for the abstract and can be removed. For example, is it important to know that the model has been developed by NOAA in the abstract?

Revised. We also changed “NOAA’s HYSPLIT” to “HYSPLIT” (not an acronym, See Stein et al., 2015).

2. Line 32: Remove capital letters from words 2-6 in the sentence starting with "Meeting...".

Per convention, the acronym (NAAQS) has been added after “National Ambient Air Quality Standards”.

3. Line 43 (or thereabouts): You need to state that HYSPLIT is a Langrangian model (and maybe elaborate on what means) as in the next paragraph you start talking about Eularian models.

Thanks for the comment. We revised the sentence.

(Line 42) “The NOAA’s HYSPLIT (Stein et al., 2015), a Lagrangian model which is designed to track air parcel trajectories, is then used to calculate transport, dispersion, and deposition of the emitted particulate matter. The SFS provides daily smoke forecasts over the continental United States, Alaska, and Hawaii to provide air-quality guidance to the public.”

4. I also notice that you don’t leave spaces between paragraphs, which makes it hard to read at times. Fix this if you can.

We are sorry for the inconvenience, but ACP template formats in such a way.

5. Line 54:You distinguish "top-down" and "bottom-up" approaches to estimating fire emissions. I think it would useful as well to discuss the advantages and disadvantages of these approaches somewhere in the introduction.

Thanks for the comment. We have added sentences for both approaches.

(Line 73) “Both bottom-up and top-down approaches have their own advantages and limitations. While the bottom-up approach may provide detailed information based on a process- or fuel-specific estimation, it relies on various surveys that require significant time and resources. On the other hand, the top-down approach relies on observations of a few atmospheric variables such as radiation or aerosol optical properties, but it has an advantage from its timely availability and geographical coverage. Both approaches complement each other for better fire emission estimation.”

6. When discussing the methodology it might be worthwhile to explicitly mention that the "inverse system" enables the calculation of fire emissions that produces an "analysis" smoke field covering the observational time window (near past to present) and that these optimal emissions are then used to fore-cast the future smoke field. I do not think this has been made explicit although it may be obvious to the expert reader.

Thanks for the comment. We have added sentences for two steps (emission inverse and forecast) for the system .

(L207) “This inverse system is designed to estimates fire emissions on the target day by analyzing past and present smoke field, and then utilizes them to forecast the future smoke field.”

7. Another point that I think needs to be made clear in the methodology section is how the experiments with different observational time windows (oday = 0, -1, 2 etc) differ from each other in the model setup. For example, for oday= 0, is it that there are no emissions prior to day 0, or is it that emissions prior to day0 are unconstrained (i.e. they use prior values), or is it that the emissions prior to day0 are in the model but they are constrained by observations on day 0 only. I suspect it is the last scenario, but this needs to be made clear. You could include this information in the paragraph starting at Line 177, which I think needs more clarity. For example, you could indicate that oday = 0 means that emissions from the model start time until day 0 (for example, November 13) are constrained by observations on day 0 only; oday= -1 means that emissions from the model start time until day 0 are constrained by observations on day 0 and day -1 (November 12) etc. As I mentioned, it is not clear that is indeed the experimental setup, but whatever it is, it needs to made clear. When you calculate the verification statistics for the oday = 0 type experiment, for example, do you include all data (for days 0, -1, -2 etc) or just data for day 0? Please make this clearer.

Thanks for the comment. Please, see the general response #1. We clarified the use of time windows for assimilation, observation and evaluation. Manuscript was also revised accordingly.

8. It would also be useful in the context of Section 3 (or elsewhere like Figure1 or in the conclusion) to say something about how the two systems (Blue Sky/Initial?and Inverse) really need to complement each other in practice. Apart from providing g the all-important first guess (or 'prior') to the inverse system, I would imagine that the Blue Sky system would also be needed to provide the first operational forecast when there are not yet any (or sufficient) observations to assimilate. In addition, in situations where there is extensive cloud cover, I would imagine that there would not be observations of smoke that could be used. This comment is related to Comment #5 above.

Thanks for the comment. This is true. Two systems complement each other. We included its importance at the manuscript.

(Line 263) "This case hints at the importance of both traditional (e.g. Blue Sky emissions) and new inverse system. They complement each other by one providing the latest data assimilation technique while the other providing a prior information and backup stability in a contaminated environment (e.g. excessive cloud cover)."

9. Line 219: The notation associated with this equation needs to be improved. Although I think I understand what you are trying to say, as it stands it is ambiguous. Firstly, it is not clear what "smoke" is supposed to be. I think you are looking at smoke mass loading, or it could be optical depth. Whatever it is, it needs to be made clear. I would use a single-letter symbol to represent the smoke variable. Since "c" is used in the first equation (Lines 148-149) that is what should be used here as well for consistency. Similarly, I would use a single letter to represent the TCM matrix coefficient (T seems like a good choice). Apart from that the equation doesn't look mathematically correct. Summing over the indices i, k, t should produce a scalar, independent of i, k, t but we know that the smoke field (mass load or optical depth) is a function of location, i, and time, t. So something is missing. I think some more work needs to be done here so that the equation makes sense.

Thanks for the comment. We modified equations.

(Line 248) "Using adjusted fire emissions, we can reconstruct the integrated smoke columns as a sum of adjusted emissions, q_{ikt}, applied to each TCM, T_{ikt}:

$$c(n,m) = \sum_{ikt} q_{ikt} \cdot T_{ikt}(n,m)$$

where *i, k* and *t* denote spatial, vertical and temporal allocation of emission sources, and *m* and *n* denote location and time of receptor (i.e. observation), respectively."

10. Line 226: change "during" to "when".

Corrected.

11. Line226: Last sentence of paragraph. Some more needs to be said here. Why is there no data on November 17? In addition, you are implying that no satellite data was used in the analysis (presumably because there was none – you must clearly state that if that is the case, and if so, why). And yet in the caption to Figure 5 we are told that a 48-hour observation time window was used. If that is the case, why could not the data for November 16 be used to constrain the analysis? Is it because your algorithm does not perform optimisation if any time steps are missing in the observational time window? You might have mentioned this elsewhere, but how frequent are the satellite observations? Every hour? Every 10 minutes?

Thanks for the comment.

ASDTA AODs are available for every hour, but some data are missing due to operational issues. We don't have control over it. In this simulation, we used 48-hour analysis. As the reviewer commented, we still have some data available to operate the inverse system. Therefore, this case demonstrated the case with limited available data. We revised manuscript to discuss the November 17 case.

(Line 259) “The November 17 output in **Figure 5** shows how the system responds when observations are limited or missing, although it still provides a robust result by honoring the initial guess information. On November 17, no ASDTA AOD was provided from the satellite operation. Under 48-hour configuration (i.e. aday=-1), the inverse system still produced reasonable outputs using limited observations (November 16) and initial guess emissions (November 16 and 17).”

12. Paragraph starting at Line 234:This is related to Comment #7. If you are using emissions initiated at the same time in all experiments in which you vary the length of observational time window, it is surprising, I think, that you get a better fit with a longer observational time window. Intuitively, all things being equal, you would expect to get a better fit with a smaller number of datapoints during the analysis. Of course, for the forecast you would expect better results with more data points during the analysis because you are less exposed to overfitting problems with more data points. It looks like you're talking about the analysis here so can you make it clearer why using data from earlier times (say day -1, -2 etc) makes the analysis better on day 0 for example? I find that a bit unclear. I can see that if you are using data from all days to calculate your forecast verification statistics and not only on the days that data is assimilated, you would get better results by using more data because you are better constraining the smoke over a longer period. If that is the case, please make it clearer which data points are included in the verification statistics.

Thanks for the comment. We strongly agree with the reviewer. In the revised manuscript, we included performance statistics with varying analysis, observation and evaluation time windows. Please, see the general response #1.

13.Paragraph starting at Line 242: When I first read this, it sounded like you are varying the vertical resolution of the sources in these experiments. But is turns out you are just varying the maximum heights of the sources. I think you should consider rewording this so that it is immediately clear what you are doing. In some sense, I think varying the vertical resolution and keeping the maximum height the same would be a more interesting experiment. Rising plumes tend to have a neutral buoyancy level at which most of the mass tends to be detrained from the plume. This is true for volcanic plumes; I don't know if it's true here. So, changing the vertical resolution may have a significant impact on the results.

Thanks for the comment. We modified wording for the vertical layer sensitivity test.

(Line 290) “To test the maximum extension, starting from two layers (i.e. with emissions released at 100 and 500 meters), we added the next higher layer over six test runs to investigate the effect of maximum extension of smoke plume. **Figure 6b** shows the results, and correlation and error statistics are summarized in **Table 3.** Including the 5000m layer,”

We also conducted more sensitivity tests of vertical layers. Please, see the general response #2.

For the detrain level of smoke plume, some wildfire smoke plumes were reported to penetrate the PBL, but generally its upward motion is less dynamic compared to volcanic plumes. We believe the maximum level of smoke plume rise is still important, and added more sensitivity tests.

14. Line 255: You must say something about the outcome of the "third test" here. Would you say coverage does not matter? Or is it better for bigger coverage (Domains 3 and 4)? If the results are inconclusive, say so.

Thanks for the comment. We have added discussion on the spatial coverage test.

(Line 306) “In most days, we have better results when we include fire emission sources at least within domain 2. It makes sense considering the effects of transported fire plumes form Mississippi and Louisiana (**Figure 3**). Maximizing geographical coverage (e.g. domain 4) did not always result in the best performance in our case study. This result, however, should be taken carefully because we do not have strong fire activities outside domain 2 in our study case. Strong long-range transport cases, typically form northwestern US, Canada and Alaska, would have bigger impacts.“

15. Line 271: You need to say something about "p" here even if briefly; for example, "p" is the persistence rate that measures...as explained further in Section xxx.

Thanks for the comment. We have added a description for p.

(Line 331) “The persistency rate, *p*, assumes the change of future day emissions. Its role will be discussed in the next Section.“

16. Lines 298-307. Given the significant uncertainty in "p", an ensemble modelling approach might be fruitful in the forecast mode. Have you looked at this? If not, it might be something you could look at in the future.

Thanks for the comment. Currently, we are considering a dynamic modeling of decaying rate based on varying weather condition. Extending the idea to ensemble approach would be an excellent idea. We will further pursue the idea. We also included this idea in the manuscript.

(Line 381) “An ensemble of HYSPLIT predictions using different meteorological inputs will be used to estimate the uncertainties of the results in the future.”

17. Line 325: What is "PM"?

PM denotes particulate matter (Line 25).

Inverse modeling of fire emissions constrained by smoke plume transport using HYSPLIT dispersion model and geostationary observations

Hyun Cheol Kim [1,2], Tianfeng Chai[1,2], Ariel Stein[1] and Shobha Kondragunta[3]

[1] Air Resources Laboratory, National Oceanic and Atmospheric Administration, College Park, MD, 20740, MD, USA
[2] Cooperative Institute for Satellite Earth System Studies, University of Maryland, College Park, MD, 20740, USA
[3] National Environmental Satellite, Data and Information Service, National Oceanic and Atmospheric Administration, College Park, MD 20740, USA

Correspondence to: Tianfeng Chai (tianfeng.chai@noaa.gov), Hyun Cheol Kim (hyun.kim@noaa.gov)

Abstract. Smoke forecasts have been challenged by high uncertainty in fire emission estimates. We develop an inverse modeling system, the HYSPLIT-based Emissions Inverse Modeling System for wildfires (or HEIMS-fire), that estimates wildfire emissions from the transport and dispersion of smoke plumes as measured by satellite observations. A cost function quantifies the differences between model predictions and satellite measurements, weighted by their uncertainties. The system then minimizes this cost function by adjusting smoke sources until wildfire smoke emission estimates agree well with satellite observations. Based on ~~NOAA's~~ HYSPLIT and ~~GOES~~Geostationary Operational Environmental Satellite Aerosol/Smoke Product (GASP), the system resolves smoke source strength as a function of time and vertical level. Using a wildfire event that took place in the Southeastern United States during November 2016, we tested the system's performance and its sensitivity to varying configurations of modeling options, including vertical allocation of emissions and spatial and temporal coverage of constraining satellite observations. Compared with currently operational BlueSky emission predictions, emission estimates from this inverse modeling system outperform in both reanalysis (21 out of 21 days; -27% average ~~RMSE~~root-mean-square-error change) and hindcast modes (29 out of 38 days; -6% average ~~RMSE~~root-mean-square-error change~~).~~) compared with satellite observed smoke mass loadings.

~~1.~~1 Introduction

Burning biomass is one of the major factors affecting global air quality (Crutzen and Andreae, 1990). Fire smoke plumes directly emit both particles that can impact cardiopulmonary health and precursors (e.g., NO_x, SO_2, NH_3, and volatile organic carbons, or VOCs) (Andreae, 2019) that react to form secondary particulate matter (PM) or other pollutants, such as ozone ~~(Dreessen et al., 2016; Jaffe and Wigder, 2012; Mok et al., 2016; Singh et al., 2012; Valerino et al., 2017)~~(Dreessen et al., 2016; Jaffe and Wigder, 2012; Mok et al., 2016; Singh et al., 2012; Valerino et al., 2017). In addition to their impact on air quality, fire emissions influence direct and indirect radiative transfer, aerosol formation, and the formation of cloud condensation nuclei, and they further interact with clouds and, eventually, with the biosphere and climate. Interaction between fire and the climate is an important factor affecting the future direction of the environment (Bowman et al., 2009).

스타일 정의: 표준: 글꼴: (영어) Times New Roman, (한글) Times New Roman, 10 pt, 영어(영국), 양쪽, 간격 단락 뒤: 0 pt, 줄 간격: 1.5줄

스타일 정의: 제목 1: 글꼴: 10 pt, 글꼴 색: 검정, 영어(영국), 글자 커닝16 pt, 양쪽, 간격 앞: 24 pt, 단락 뒤: 12 pt, 다단계 번호 매기기 + 수준:1 + 번호 스타일: 1, 2, 3, … + 시작 번호: 1 + 맞춤: 왼쪽 + 맞춤 위치: 0" + 들여쓰기 위치: 0.3", 다음 단락과의 사이에 페이지 나누지 않음

스타일 정의: 머리글: 글꼴: (영어) Times New Roman, (한글) Times New Roman, 10 pt, 영어(영국), 양쪽, 줄 간격: 1.5줄, 탭: 3.15", 가운데 + 6.3", 오른쪽 + 3.25"(없음) + 6.5"

스타일 정의: 하이퍼링크

스타일 정의: 풍선 도움말 텍스트: 글꼴: (영어) Tahoma, (한글) Times New Roman, 8 pt, 영어(영국), 양쪽

스타일 정의: 캡션: 글꼴: (영어) Times New Roman, (한글) Times New Roman, 굵게, 기울임꼴 없음, 글꼴 색: 자동, 영어(영국), 양쪽

스타일 정의: 바닥글: 글꼴: (영어) Times New Roman, (한글) Times New Roman, 10 pt, 영어(영국), 양쪽, 탭: 3.13", 가운데 + 6.27", 오른쪽 + 3.25"(없음) + 6.5"

스타일 정의: 메모 텍스트

스타일 정의: 수정

스타일 정의: 일반 (웹)

서식 있음: 왼쪽: 0.65", 오른쪽: 0.65", 위: 0.39", 아래: 0.93", 너비: 8.27", 높이: 9.45", 머리글의 가장자리와의 간격: 0", 바닥글의 가장자리와의 간격: 0.51", 텍스트와의 간격: 0.16"

서식 있음: MS title, 왼쪽, 간격 앞: 0 pt

서식 지정함: 글꼴: 17 pt

서식 지정함: 글꼴: 12 pt

서식 지정함: 위 첨자

서식 지정함: 위 첨자/아래 첨자없음

서식 있음: 간격 앞: 0 pt

서식 지정함: 글꼴: 굵게 없음

서식 있음: 제목 1, 간격 앞: 0 pt, 글머리 기호 또는 번호 없이

서식 있음: 간격 앞: 0 pt

서식 있음: 가운데

While high fire activities are affected by decadal-scale variation of the climate (Carvalho et al., 2011; Flannigan et al., 2005; Spracklen et al., 2009), aerosols released from fires and changed surface albedo due to burnt areas are influential, as they disturb the radiative balance in the atmosphere (Liu et al., 2014).

Meeting National Ambient Air Quality Standards (NAAQS) requires U.S. state agencies to understand the primary emission sources for particulate matter. Notwithstanding many states' continuous efforts to control in-state sources of pollutants, it is challenging to account accurately for fire emissions and the out-of-state transport of fire plumes. Due to the huge impact of fires on regional air quality, accurately forecasting their impact is an important public-service task, performed mostly by government agencies. The National Oceanic and Atmospheric Administration (NOAA) Smoke Forecasting System (SFS) was initiated after the large wildfire event in May 1998 (In et al., 2007; Rolph et al., 2009), to predict the movement of smoke from large wildfires (Rolph et al., 2009; Stein et al., 2009). The SFS uses the National Environmental Satellite, Data, and Information Service (NESDIS) Hazard Mapping System (HMS) (Ruminski and Kondragunta, 2006) and the U.S. Forest Service's (USFS) BlueSky framework (Larkin et al., 2009) to detect fires and estimate emissions. The NOAA's HYSPLIT (Stein et al., 2015) ~~model~~, a Lagrangian model which is designed to track air parcel trajectories, is then used to calculate transport, dispersion, and deposition of the emitted particulate matter. The ~~system~~SFS provides daily smoke forecasts over the continental United States, Alaska, and Hawaii to provide air-quality guidance to the public.

Eulerian systems are also used for smoke forecasting. Smoke emissions from wildfires have been incorporated into the NOAA's National Air Quality Forecast Capability system as real-time, intermittent sources; this system has been forecasting regional air quality for surface ozone and particulate matter concentration since 2015 ~~(Lee et al., 2017)~~(Lee et al., 2017). The High-Resolution Rapid Refresh Smoke (HRRR-smoke; https://rapidrefresh.noaa.gov/hrrr/) (Ahmadov et al., 2017) system also provides 36-hour forecasts for the continental United States using the WRF-Chem modeling system with emissions derived from satellite-measured fire radiative power (FRP). Also, ~~Chen et al. (2019)~~Chen et al. (2019) demonstrated an air quality forecast system over Canada that incorporates near-real-time measurement of biomass burning emissions to forecast smoke plumes from fire events. There are numerous other global smoke forecast systems ~~(Chen et al., 2011; Larkin et al., 2009; Lee et al., 2019; Li et al., 2019; Pavlovic et al., 2016; Sofiev et al., 2009)~~(Chen et al., 2011; Larkin et al., 2009; Lee et al., 2019; Li et al., 2019b; Pavlovic et al., 2016; Sofiev et al., 2009).

Any improved smoke forecast system must confront several uncertainties, particularly fire (especially wildfire) emission amounts and their allocation spatially and vertically. In general, fire emissions may be estimated in one of two ways: bottom up and top down. Regarding the more traditional bottom-up approaches, fuel consumption is estimated as the product of burnt size, pre-burn fuel loading of the fire-affected area, completeness of combustion, and emission factors (Seiler and Crutzen, 1980). Since emission factors are specific to the type of tree ablaze, a completely constructed database is very important in this approach. For example, Wiedinmyer et al. (2006), in estimating emissions from fires in North America, estimated fuel loading based on a combination of satellite and ground-collected data, such as Moderate Resolution Imaging Spectroradiometer (MODIS) thermal anomalies, the Global Land Cover Characteristics dataset, the MODIS Vegetation Continuous Fields Product, and emission factors.

서식 있음: 가운데

Recently, the global coverage of space-borne instruments has encouraged top-down approaches. A fire's heat signature (that is, FRP) is detectable by satellite, and FRP can be used to estimate the rate of combustion (Giglio et al., 2003; Kaufman et al., 1998). Measurements of FRP from polar-orbiting sensors can both detect active fires and characterize their properties (Freeborn et al., 2009; Jordan et al., 2008; Schroeder et al., 2014). FRP data have been used to quantify biomass consumption, detect the locations of fire emission sources, trace gas and aerosol production ~~(Ellicott et al., 2009; Kaiser et al., 2012a; Vermote et al., 2009)~~(Ellicott et al., 2009; Kaiser et al., 2012; Vermote et al., 2009), and estimate the vertical extension of smoke plumes and other fire emissions (Val Martin et al., 2010). Several global fire emission databases (e.g., Global Fire Emissions Database (GFED), Fire Inventory form NCAR (FINN), Quick Fire Emissions Database (QFED), Global Fire Assimilation System (GFAS), Fire Energetics and Emissions Research (FEER), and Global Biomass Burning Emissions Product (GBBEP)) have been developed using one or both the bottom-up and top-down approaches ~~(Ichoku and Ellison, 2014; Kaiser et al., 2012b; van der Werf et al., 2010; Wiedinmyer et al., 2011; Zhang et al., 2012).~~(Ichoku and Ellison, 2014; Kaiser et al., 2012; van der Werf et al., 2010; Wiedinmyer et al., 2011; Zhang et al., 2012). Both bottom-up and top-down approaches have their own advantages and limitations. While the bottom-up approach may provide detailed information based on a process- or fuel-specific estimation, it relies on various surveys that require significant time and resources. On the other hand, the top-down approach relies on a few simple observations of radiation or aerosol optical property, but it has an advantage from its timely availability and geographical coverage. Both approaches complement each other for better fire emission estimation.

~~This study extends the current capabilities of the NOAA SFS fire smoke forecast systems, most of which estimate fire emissions using the surface and thermal characteristics of detected fire locations. Transport pathways of smoke plumes are rarely considered (e.g. Nikonovas et al., 2017) in determining emissions strength, vertical extension, and temporal variation. This study aims to develop an inverse modeling system for fire emissions based on a Lagrangian model that can resolve these transport pathways using HYSPLIT simulations and satellite observations.~~
This study extends the current capabilities of the NOAA SFS fire smoke forecast systems, most of which estimate fire emissions using the surface and thermal characteristics of detected fire locations. Transport pathways of smoke plumes are rarely considered in determining emissions strength, vertical extension, and temporal variation. This study aims to develop an inverse modeling system for fire emissions based on a Lagrangian model that can resolve these transport pathways using HYSPLIT simulations and satellite observations. Such an approach has been adapted to estimate inversely various emission sources, including greenhouse gas emissions (Kunik et al., 2019; Nickless et al., 2018; Turnbull et al., 2019), volcanic ashes and sulfur dioxide emissions (Boichu et al., 2014; Crawford et al., 2016; Zidikheri and Lucas, 2020), and radionuclide release from nuclear power plant incident (Chai et al., 2015; Katata et al., 2015; Li et al., 2019a), but was rarely used in fire emission estimation (e.g. Nikonovas et al., 2017).

The remainder of the paper is structured as follows. Section 2 describes the model and satellite data used to detect fire locations and the transport of fire smoke. Section 3 concerns the methodology and structural design of the inverse modeling system. Results from a case study, sensitivity tests, and comparison with the currently operational system are presented in Section 4. Finally, Section 5 summarizes and discusses directions for future work.

서식 있음: 간격 앞: 0 pt

서식 있음: 가운데

~~2.~~2 Data

~~2.1.~~2.1 HMS and BlueSky

Consistent with the NOAA SFS system, the HMS data is utilized to detect wildfire information. HMS, developed as a tool to identify fires and their smoke emissions over North America in an operational environment, incorporates images from multiple geostationary and polar-orbiting environmental satellites, including Geostationary Operational Environmental Satellite (GOES)-East/West, Suomi-National Polar-orbiting Partnership (NPP), MODIS, and Advanced Very High Resolution Radiometer (AVHRR) METOP-B, to provide the location and time of detected fires. Automated fire detection algorithms are first employed for each sensor, and then human analysts apply further quality control by examining visible channel imagery for false alarms and missed hotspots (Ruminski et al., 2008; Ruminski and Kondragunta, 2006; Schroeder et al., 2008).

The BlueSky system, developed by the U.S. Forest Service, provides the first guess for fire emission estimation. ~~A~~As a modeling framework, BlueSky links several models of fire information, fuel loading, fire consumption, fire emissions, and smoke dispersion (Larkin et al., 2009; Strand et al., 2012). For the original NOAA SFS system, BlueSky emissions are used as inputs for the dispersion model. In this study, we use the BlueSky emission rate as an initial guess before applying the inverse modeling system.

~~2.2. GASP~~

~~The GOES Aerosol/Smoke Product (GASP) is a retrieval of the aerosol optical depth (AOD) using GOES visible imagery (Kondragunta et al., 2008; Prados et al., 2007). This product is available at 30-minute intervals and 4 km × 4 km spatial resolution during the sunlit portion of the day. The Automated Smoke and Tracking Algorithm (ASDTA; https://www.ssd.noaa.gov/PS/FIRE/ASDTA/asdta_west.html) detects smoke associated with detected fire source locations. A pattern-recognition technique is used for plumes transported far from fire sources. The GASP product is particularly useful for tracking fast-moving plumes, which polar-orbiting sensors often cannot detect since they provide only one daily image. Since the ASDTA product is a part of the GASP product, in this study, GASP and ASDTA indicate total AOD and smoke AOD, respectively.~~

2.2 GASP

The GOES Aerosol/Smoke Product (GASP) is a retrieval of the aerosol optical depth (AOD) using GOES visible imagery (Kondragunta et al., 2008; Prados et al., 2007). This product is available at 30-minute intervals and 4 km × 4 km spatial resolution during the sunlit portion of the day. The Automated Smoke and Tracking Algorithm (ASDTA; https://www.ssd.noaa.gov/PS/FIRE/ASDTA/asdta_west.html) detects smoke associated with detected fire source locations. For each pixel, the radiative signatures of an aerosol layer (e.g. dust and smoke) are determined by the scattering and absorption properties of the aerosol. ASDTA also utilizes a pattern-recognition technique to isolate smoke aerosols from other type of aerosols, so it can recognize plumes transported far from fire sources. The GASP product is particularly useful for tracking fast-moving plumes, which polar-orbiting sensors often cannot detect since they provide only one daily image.

서식 있음: 제목 1, 간격 앞: 0 pt, 글머리 기호 또는 번호 없이

서식 있음: 지정한 문자 수에 맞춰 오른쪽 들여쓰기 자동 조정, 간격 앞: 0 pt, 한글과 영어 간격을 자동으로 조절, 한글과 숫자 간격을 자동으로 조절

서식 있음: 가운데

Since the ASDTA product is a part of the GASP product, in this study, GASP and ASDTA indicate total AOD and smoke AOD, respectively. Hourly data were used for the inverse system.

~~2.3.~~2.3 HYSPLIT

HYSPLIT computes air parcel trajectories and the dispersion or deposition of atmospheric pollutants (Stein et al., 2015). It has been widely used to simulate pollutant events, including volcanic ash, smoke from wildfires, radioactive nuclei dispersion, and emissions of anthropogenic pollutants. For the inverse modeling system, we used the Transfer Coefficient Matrix (TCM) approach. The unit source calculations give the dispersion factors from the release point for every emission period to each downwind grid location, defining what fraction of emissions are transferred to each location varying as a function of time. This is defined as the TCM (Draxler and Rolph, 2012). The TCM is computed for inert and depositing species and, when quantitative air concentration results are required, the final air concentration is computed in a simple post-processing step that multiplies the TCM by the appropriate emission rate ~~and radioactive decay constant.~~ Results for multiple emission scenarios are easily created and may be used to optimize model results as more measurement data become available.

For the inverse system, 120-hour HYSPLIT simulations were conducted daily, starting from 6Z using North American Model 12-km meteorology~~, at each fire source location provided by the HMS fire detection information. Fifty thousand particles were released for each simulation, and dispersed concentrations were vertically integrated up to 5000m onto 0.1 degree spatial grids. In this paper the integrated mass loading of particles from HYSPLIT simulation and satellite products will be compared with each other. For satellite products (e.g., GASP, ASDTA, and MODIS), smoke is converted from AOD using a simple conversion factor (i.e. 1 AOD = 0.25 g/m^2) which is compatible to 4 m^2/g mass extinction efficiency (Nikonovas et al., 2017).~~ (NAM12), at each fire source location provided by the HMS fire detection information. Fifty thousand particles were released for each simulation, and dispersed concentrations were vertically integrated up to 5000m onto 0.1 degree spatial grids. Hourly outputs were integrated to match with satellite observational data. HYSPLIT modelling options were configured to be consistent with the SFS system, including options for dry and wet depositions (i.e. 0.8 μm diameter with 2 g/cm^3 density) (Rolph et al., 2009). In this paper the integrated mass loading of particles from HYSPLIT simulation and satellite products will be compared with each other. For satellite products (e.g., GASP, ASDTA, and MODIS), smoke is converted from AOD using a simple conversion factor (i.e. 1 AOD = 0.25 g/m^2) which is compatible to 4 m^2/g mass extinction efficiency (Nikonovas et al., 2017). Although we used a simple conversion factor for the study, it varies in time and space (i.e. 3.9 – 5.3 m^2/g) (Chand et al., 2006; Hobbs et al., 1996; Ichoku and Ellison, 2014; Nikonovas et al., 2017; Reid et al., 2005). Therefore, applying more realistic conversion factors and their uncertainties into the system would be another factor in the future improvement of the system.

For HYSPLIT runs, smoke indicates the sum of dispersion simulations (i.e. TCM runs in concentration unit) multiplied by emissions for each source. Since we have integrated dispersion model outputs (in density unit) up to 5000m height, the

서식 있음: 제목 2, 간격 앞: 0 pt, 글머리 기호 또는 번호 없이

서식 있음: 간격 앞: 0 pt

서식 있음: 가운데

results shown in the study are obtained by multiplying the column height (i.e. 5000m) and demonstrated as total mass loading for a column (kg/m^2).

~~3.~~3 Methodology

~~3.1.~~3.1 Overview

A HYSPLIT inverse system was built and successfully applied to estimate the cesium-137 releases from the Fukushima Daiichi Nuclear Power plant accident in 2011 (Chai et al., 2015). It was then modified to estimate the volcanic ash source strengths, vertical distribution, and temporal variations by assimilating MODIS satellite retrievals of volcanic ash clouds while using ash cloud top height information as well (~~Chai et al. (2017)~~Chai et al., 2017). It was found that simultaneously assimilating observations at different times produces better hindcasts than only assimilating the most recent observations. In this application, the HYSPLIT-based Emissions Inverse Modeling System for wildfires (HEIMS-fire) is designed to assimilate satellite observations to generate wildfire emission estimates. The smoke plume transport and dispersion, captured by frequent geostationary satellite retrievals, can be used as constraints to obtain the smoke emission estimates. In the system, a cost function quantifies the differences between HYSPLIT model predictions and satellite-observed AOD, weighted by model and observation uncertainties. Minimizing the cost function by adjusting emission rates at different fire locations and at several different release heights thereby provides the fire emission estimates.

~~3.2.~~3.2 Cost function

Taking a top-down approach, unknown emission terms are obtained by searching for the emissions that provide the model predictions that most closely match the observations. With fire locations mostly identified by the HMS system, unknown emission rates at these specified locations remain undetermined. At each fire location, released smoke can reach different heights under various fuel-loading and meteorological conditions. In addition, emission rates may vary significantly with time. Thus, the unknown elements of the inverse problem are the emission rates q_{ikt} at each wildfire location i at different heights k and time periods t. The cost function F is defined as:

$$F = \frac{1}{2}\sum_{t=1}^{T}\sum_{k=1}^{K}\sum_{i=1}^{I}\frac{(q_{ikt} - q_{ikt}^{b})^2}{\sigma_{ikt}^2} + \frac{1}{2}\sum_{n=1}^{N}\sum_{m=1}^{M}\frac{(c_{nm}^{h} - c_{nm}^{o})^2}{\varepsilon_{nm}^2} + F_{other}$$

where c_{nm}^{o} is the m-th gridded satellite observation (e.g., GASP ASDTA smoke mass loading) at time period n, and c_{nm}^{h} is its HYSPLIT counterpart.

A background term is included to measure the deviation of the emission estimate from its first guess, q_{ikt}^{b}, obtained from the operational BlueSky emission computation. The background term ensures the problem remains well-posed even with the

서식 있음: 제목 1, 간격 앞: 0 pt, 글머리 기호 또는 번호 없이
서식 있음: 간격 앞: 0 pt
서식 있음: 제목 2, 간격 앞: 0 pt, 글머리 기호 또는 번호 없이
서식 있음: 간격 앞: 0 pt
서식 지정함: 글꼴 색: 자동
서식 지정함: 글꼴 색: 자동
서식 있음: 간격 앞: 0 pt
서식 지정함: 글꼴 색: 자동
서식 지정함: 글꼴 색: 자동
서식 지정함: 글꼴 색: 자동
서식 지정함: 글꼴 색: 자동
서식 지정함: 글꼴 색: 자동
서식 지정함: 글꼴 색: 자동
서식 지정함: 글꼴 색: 자동
서식 지정함: 글꼴 색: 자동
서식 지정함: 글꼴 색: 자동
서식 지정함: 글꼴 색: 자동
서식 지정함: 글꼴 색: 자동
서식 지정함: 글꼴 색: 자동
서식 있음: 가운데

limited observations available in certain circumstances. The background error variance σ^2_{ikt} measures uncertainties in q^b_{ikt}. ~~The observational error variances, ε^2_{nm}, represent uncertainties in both the model and observations, as well as the representative errors. F_{other} refers to the other regularized terms that can be included in the cost function.~~Pan et al. (2020) compared six global emission estimates and found that the total emission differs by a factor of 3.8. However, emission estimations at specific locations and times can have much larger errors. In addition, the vertical distribution of the smoke emissions is difficult to determine and this adds even more uncertainties to the emission estimates. We chose a large uncertainty for the background term as $\sigma_{ikt}=1000\times q^b_{ikt}+ 1000$ kg/hr at all locations and heights to minimize the adverse impact of inaccurate BlueSky emission estimates. The observational error variances, ε^2_{nm}, represent uncertainties in both the model and observations, as well as the representative errors. Kondragunta et al. (2008) indicated that GOES aerosol retrievals over land were expected to have uncertainties within $0.15\tau \pm 0.05$, where τ is the AOD. Paciorek et al. (2008) showed a better performance of GOES aerosol retrievals in eastern U.S. than in western U.S. Green et al. (2009) demonstrated that GOES AOD correlates best with AERONET in autumn (September to November) than in other seasons. They showed that the RMS error was 0.060 in autumn while the average for all seasons is 0.0149. Considering the better performance in the Eastern US and in November, AOD uncertainties of $0.10\tau \pm 0.06$ are assumed in this paper. A slightly larger additive component of the AOD error is chosen to include the effects of the representative errors and model errors which do not vary with the observed AOD values. F_{other} refers to the other regularized terms that can be included in the cost function. For instance, Chai et al. (2015) has a temporal smoothness penalty term to avoid abrupt changes in the temporal profile of the release rates. While this optimization problem could be solved to obtain optimal emission estimates using many minimization tools, we used the Limited-Memory Broyden–Fletcher–Goldfarb–Shanno (BFGS) algorithm (Zhu et al., 1997).

~~3.3.~~3.3 Inverse system

The HEIMS-fire system is designed to conduct a two-step operation: (1) estimation of fire emission using an inverse system, and (2) forecast modeling of fire smoke using estimated fire emissions. The inverse system utilizes observations and modeling systems available from multiple agencies. We aim to estimate objectively and optimally wildfire smoke sources' strength, vertical distribution, and temporal variations by assimilating GASP AODs. ~~Figure 1~~**Figure 1** summarizes the system's incremental stages of data processing, listed below with the required data (and their providing agencies):

(1) Fire detection: Hazard Mapping System (NESDIS)
(2) HYSPLIT simulations with unit emissions at different locations and release heights
(3) Construction of Transfer Coefficient Matrix with available observations
(4) Initial guess for fire emissions (BlueSky, U.S. Forest Service)
(5) Cost function minimization to estimate smoke emissions
(6) Smoke forecast using adjusted smoke emissions

서식 지정함: 글꼴 색: 자동
서식 지정함: 글꼴 색: 자동
서식 지정함: 글꼴 색: 자동
서식 지정함: 글꼴 색: 자동
서식 지정함: 글꼴 색: 자동
서식 지정함: 글꼴 색: 자동
서식 지정함: 글꼴 색: 자동
서식 지정함: 글꼴 색: 자동
서식 지정함: 글꼴 색: 자동
서식 있음: 제목 2, 간격 앞: 0 pt, 글머리 기호 또는 번호 없이
서식 있음: 간격 앞: 0 pt
서식 지정함: 글꼴: 굵게
서식 있음: 왼쪽
서식 있음: 가운데

By minimizing a cost function, the HEIMS-fire system provides adjusted fire emissions that can describe realistic smoke plumes. Results in the following section show that the assimilated smoke plumes agree well with satellite observations. The system requires as input a first guess before it can start to minimize the cost function. Selection of this input is usually critical both for the performance of the minimization calculation and for the final output.

We also explain here the naming conventions for temporal coverage of emission estimation processes and forecasting processes. ~~Observational~~This inverse system is designed to estimate fire emissions on the target day by analyzing past and present smoke field, and then utilizes them to forecast the future smoke field. The assimilation days (i.e. ~~oday~~aday = 0,-1,-2) (see **Figure S1**) indicate the temporal coverage of dispersions and constraining ~~observational days.~~observations. For ~~example, fire emissions on~~ a target day of November 13~~ can be estimated~~, inversions are conducted using HYSPLIT dispersion simulations and ASDTA observations for 24 hours (i.e. ~~oday~~aday=0), 48 hours (i.e. ~~oday~~aday=-1), 72 hours (i.e. ~~oday~~aday=-2), and 96 hours (i.e. ~~oday~~aday=-3). Estimated fire emissions are used to simulate fire smoke for November 13 (i.e. fday=0; reanalysis), and the same amount of fire emissions are used in forecast mode for November 14 (i.e. fday=+1) and 15 (i.e. fday=+2). Application of forecast mode will be further discussed in Section 4.5.

~~4.~~4 Results

~~4.1.~~4.1 Case study

A case study using a November 2016 wildfire event was conducted to test the performance of the HEIMS-fire system. This fire event was a series of wildfires in the southeastern United States in October and November 2016. The U.S. Forest Service reported at least 80,000 acres burned from October 23 to December 9, 2016. For the case study, we focused on the fire event that occurred in Georgia, South Carolina, North Carolina, and the adjacent states from November 10 to 17, 2016. ~~**Figure 2**~~**Figure 2** shows an example of fire smoke detected from MODIS true-color ~~channel~~image and three AOD products from MODIS, GASP, and ASDTA on November 10, 2016. Wildfires in the Appalachians of northern Georgia, western North Carolina, and eastern Tennessee began to produce large smoke plumes moving southeast. Numerous smoke plumes could be seen from active wildfires burning across the region. Changes in the fire events from November 8 to 19, 2016, are also shown as MODIS truecolor images in supplementary materials (**Figure S2**).

~~4.2.~~4.2 Model configuration

The month of November 2016 saw fires nationwide, although the most extensive fires happened in the southeastern U.S. region. We considered four geographic domains in determining fire source inputs, as shown in ~~**Figure 3.**~~**Figure 3**. Red dots indicate HMS fire detections during November 2016. The results of the sensitivity test using these domains are discussed in Section 4.4.

The inverse modeling system was tuned using various sensitivity tests. A series of twin experiments was conducted to test the range of uncertainties that comes from the system design. A twin experiment is an idealized modeling test in which we

서식 있음: 간격 앞: 0 pt

서식 있음: 제목 1, 간격 앞: 0 pt, 글머리 기호 또는 번호 없이

서식 있음: 간격 앞: 0 pt

서식 지정함: 글꼴: 굵게

서식 있음: 제목 2, 간격 앞: 0 pt, 글머리 기호 또는 번호 없이

서식 있음: 간격 앞: 0 pt

서식 지정함: 글꼴: 굵게

서식 있음: 가운데

assume that the modeled world adeptly mimics the real world. Using a true solution for the situation, we can test the system's capability to reproduce the true answer. We tested uncertainties of the system across multiple scenarios and four types of potential uncertainty (vertical allocation, temporal coverage, spatial coverage, and impact of observation errors) in these twin experiment cases. Detailed descriptions of the twin experiments and sensitivity test will be made available in a separate paper (See supplementary information).

~~4.3.~~4.3 Emission estimation

Fire emissions and their vertical distributions for each detected fire location were estimated using the HEIMS-fire system, inversely modeled from ASDTA AOD data as described above. Locations and times of fires detected by HMS were used to initiate HYSPLIT simulations, with emissions released over six layers (100, 500, 1000, 1500, 2000, and 5000 m). On November 11, 46 fire locations were identified within the assimilation domain (domain 1 in ~~Figure 3)~~ **Figure 3**). Thus, the TCM was established based on 276 HYSPLIT simulations (46 fires × 6 release altitudes) and GASP AOD observations. Emissions rates calculated from the BlueSky system were used as an initial condition. Emissions were evenly distributed to all layers used in the system.

Minimizing the cost function results in the estimation of ~~assimilated~~ fire emissions. ~~Figure 4~~**Figure 4** shows the agreement between the modeled and observed mass loading from the initial to the adjusted emission estimates. ~~Table 1~~**Table 1** presents summary statistics for the changes in reconstructed smoke mass loading from the initial guess to the adjusted emissions. In the end, estimated fire emissions were combined to reconstruct fire smoke plumes. Using adjusted fire emissions, we can reconstruct the integrated smoke columns as a sum of adjusted emissions, q_{ikt}, applied to each ~~TCM_{ikt}~~TCM, T_{ikt}:

$$\sim\!\sim Smoke = \sum_{ikt} q_{ikt} \cdot TCM_{ikt} \sim\!\sim$$

$$c(n,m) = \sum_{ikt} q_{ikt} \cdot T_{ikt}(n,m)$$

where ~~I~~*i*, *k* and *t* denote spatial, vertical and temporal allocation~~,~~ of emission sources, and *m* and *n* denote location and time of receptor (i.e. observations), respectively. ~~Figure 5~~**Figure 5** presents the spatial distribution of reconstructed fire smoke mass loading for the case study in terms of column integrated density. We applied estimated fire emissions to TCM runs for each detected fire location and vertical release height and then merged them into one hourly concentration field. Reconstructed smoke plumes (i.e., integrated dispersion outputs in 0-5000m height) show a good agreement with observed smoke (~~Figure 5)~~**Figure 5**). The first and second columns compare ASDTA and HEIMS smokes for spatially and temporally matching pixels, and the third column shows ~~that fully~~the full spatial coverage of HEIMS smoke for daytime (around 8AM-5PM local time) ~~during~~when ASDTA data is available. The November 17 output shows how the system responds when observations are limited or missing, although it still provides a robust result by honoring the initial guess information. On November 17, no ASDTA AOD is available and emission estimates for the day was done using only November 16 observations under 48-hour configuration (i.e. aday=-1). While it still generates reasonable results for

서식 있음: 제목 2, 간격 앞: 0 pt, 글머리 기호 또는 번호 없이
서식 있음: 간격 앞: 0 pt
서식 지정함: 글꼴: 굵게
서식 지정함: 글꼴: 굵게
서식 지정함: 글꼴: 굵게
서식 지정함: 글꼴: 굵게
서식 있음: 간격 앞: 0 pt
서식 지정함: 글꼴: 굵게
서식 지정함: 글꼴: 굵게
서식 지정함: 글꼴: 굵게
서식 있음: 가운데

available data (i.e. data from November 16. See **Figure 4**), it happened to cause a seriously bias on November 17 simulation (**Figure S3**). We adjusted the system to weigh initial guess more if available observations are lacking seriously. This case hints at the importance of both traditional (e.g. Blue Sky emissions) and new inverse system. They complement each other by one providing the latest data assimilation technique while the other providing a prior information and backup stability in a contaminated environment (e.g. excessive cloud cover).

~~4.4.~~4.4 Sensitivity tests

Similar to the twin experiments, which, as noted above, we will report in a forthcoming paper, we conducted a series of sensitivity tests to investigate how the inverse model responds to changes in input data and various configurations of the modeling framework. This will be achieved by focusing on variation in temporal coverage, spatial coverage, and vertical allocation of smoke plumes.

First, we changed the ~~use of observational data to constrain fire emissions~~assimilation time windows from one (24-hours) to four days (96-hours). Since the impact of fire emissions easily translates over multiple days, we tested how temporal coverage affects system results. The 'one-day' (~~oday~~aday=0) simulation is run through the inverse model using ~~dispersion~~dispersions and observations for the target day, while the 'two-day' simulation uses two days (i.e., 48 hours) of ~~dispersion~~dispersions and observations (~~oday~~aday=-1). For this test, all observations within the assimilation time windows were selected for the assimilation and the evaluation. The results are shown in ~~**Figure 6**~~**Figure 6a**, while the correlation and error statistics are summarized in ~~**Table 2.**~~the top section of **Table 2** (i.e. [A:24h, O:24h, E:24h], … , [A:96h, O:96h, E:96h]). With the exception of November 10 and 11, in the early stage of the fire event, both the correlation coefficient (R) and normalized root-mean-square error (~~RMSE~~NRMSE) were improved by the use of more days (i.e., three or four days) of ~~dispersion~~dispersions and observations for the inverse model. This makes sense, because emissions from multi-day fire events spread out and affect concentrations over proceeding days.

A series of additional simulations were also conducted to test the system's sensitivity to the selection of observations for the assimilation and the evaluation. In these tests, we investigated combinations in assimilation time ("A" in **Table 2**), observational time ("O") and evaluation time windows ("E"). Results are also summarized in **Table 2**. For a fixed assimilation time period (i.e. [A:96h]), using shorter observational time window resulted in a better result. This makes sense because we expect a better fitting with smaller number of data points. However, it can be easily exposed to overfitting problem if available data for the assimilation is too small.

Second, we tested the layers at which ~~smoke dispersions~~fire emissions are initiated in the model. As expected, including more layers results in better statistics, since the transport and dispersion of each smoke plume can vary with the altitude to which their fire emissions are allocated. We tested the model's ~~uncertainty~~uncertainties on layers' maximum extension and resolution, with varying selections of two to seven layers at 100, 500, 1000, 1500, 2000, 5000, or 10000 meters. ~~Starting~~To test the maximum extension, starting from two layers~~,~~ (i.e. with emissions released at 100 and 500 meters~~,~~), we added the next higher layer over six test runs~~.~~ to investigate the effect of maximum extension of smoke plume. ~~**Figure 6**~~**Figure 6b**

서식 지정함: 글꼴: 굵게

서식 지정함: 글꼴 색: 빨강

서식 있음: 제목 2, 간격 앞: 0 pt, 글머리 기호 또는 번호 없이

서식 있음: 간격 앞: 0 pt

서식 지정함: 글꼴: 굵게

서식 지정함: 글꼴: 굵게 없음

서식 지정함: 글꼴: 굵게

서식 지정함: 글꼴: 굵게

서식 있음: 간격 앞: 0 pt

서식 지정함: 글꼴: 굵게

서식 지정함: 글꼴: 굵게

서식 있음: 가운데

shows the results, and correlation and error statistics are summarized in ~~**Table 3.** As expected, including more layers generally produce better result~~**Table 3**. Including the 5000m layer, especially, resulted in noticeable change, implying the potential benefit of including high-level transport for specific days. Since 5000m layer is above typical planetary boundary layer height, emissions injected at this level experience different physical characteristics. Smoke lofted into the free troposphere is less affected by turbulence and scavenging, and transports easily hundreds or thousands of kilometers downwind because of the higher wind speeds. Addition of 5000m layer would represent well the potential long-range transport. Smoke plume rise is one of traditionally importation questions in smoke modelling, so further research on the topic is warranted. Effects of the layer resolution were also tested. Starting from two layers (i.e. 100m and 5000m), we added intermediate layers up to six layers, and evaluated their performances (**Table S3**). As expected, including more layers resulted in the better result, but its improvement was not dramatic after four layers.

In the third test, we varied the spatial coverage of input fire information. Although wildfire impacts easily spread by long-range transport, we could not include all the global fire information due to limited computational resources. We therefore tested different spatial domains of fire locations to evaluate what spatial coverage of wildfire detection information is required to estimate fire emissions. ~~To enable comparison, we fixed the coverage for the observational data that are used to constrain the system. **Figure 6c** and **Table 4**~~Fire sources from domain 1-4 (**Figure 3**) were used in the assimilation constrained by ASDTA AOD inside Domain 1. **Figure 6**c and **Table 4** show correlation and error statistics from the sensitivity test of spatial coverage. ~~We tested the inverse system by changing the number of fire detection inputs inside the four domains denoted in **Figure 3**. To constrain and evaluate all sensitivity tests, we used ASDTA AOD only inside Domain 1.~~In most days, we have better results when we include fire emission sources at least within domain 2. It makes sense considering the effects of transported fire plumes form Mississippi and Louisiana (**Figure 3**). Maximizing geographical coverage (e.g. domain 4) did not always result in the best performance in our case study. This result, however, should be taken carefully because our study case may not represent a strong long-range transport case of fire smokes.

~~4.5.~~4.5 Hindcast and operation

In this section, we conducted a HEIMS system for hindcast mode, and compared it with operational products from the SFS system. Both SFS and HEIMS use fire detection from HMS for consistency, and HEIMS uses SFS fire emissions for initial guess information. SFS simulates 72-hour dispersion of fire smoke for every day in November 2016, which is consistent with fday=0,+1,+2 of the HEIMS hindcast simulations (as described in **Figure S1**).

Notable differences in the configuration of SFS and HEIMS are plume rise estimation ~~and~~, temporal resolution of fire emissions, fire decaying assumption, and meteorology. While SFS computes plume rise using the Briggs' equation (Arya, 1998; Briggs, 1969), which assumes an air parcel's rise is based only on the buoyance terms, HEIMS determines fire emissions' vertical allocation using an inverse system. At the initial guess, SFS fire emissions are evenly distributed in all layers. Current HEIMS assumes daily emission variation compared to hourly emissions of SFS. Also, SFS assumes 75% of emissions still happen at the same location the next day, the HEIMS uses 50% decay assumption after sensitivity tests, which

서식 지정함: 글꼴: 굵게

서식 지정함: 글꼴: 굵게

서식 지정함: 글꼴: 굵게

서식 지정함: 글꼴: 굵게

서식 지정함: 글꼴: 굵게

서식 있음: 제목 2, 간격 앞: 0 pt, 글머리 기호 또는 번호 없이

서식 있음: 간격 앞: 0 pt

서식 있음: 가운데

will be discussed in the next section. For HEIMS simulation, we used ~~oday~~aday=-1 (two-day temporal coverage) for the simulations shown. On the other hand, HEIMS would be benefitted with a better meteorology. Although both systems use the NAM12 meteorology, HEIMS hindcast meteorology should be better because we only have the first days of forecast archives.

For forecasting days, smoke is estimated as the summation of impact from previous days and new emissions on the target days. For example, smoke at fday=+2 can be reconstructed as

$$S_{fday=+2} = q_{f=0} \cdot TCM_{f=0} + q_{f=0} \cdot p \cdot TCM_{f=+1} + q_{f=0} \cdot p^2 \cdot TCM_{f=+2}$$

where q and p denote emissions and persistency rate, respectively. The persistency rate, p, assumes the change of future day emissions. Its role will be discussed in the next Section.

~~Figure 7~~ and ~~Figure 8~~**Figure 7** and **Figure 8** demonstrate simulated fire smoke by SFS and HEIMS on Nov. 11 and two-day forecasts (hindcasts for HEIMS) for Nov. 12 and 13. Both systems reproduced well the smoke in their general patterns and intensity, as shown in ASDTA AOD and MODIS truecolor image (~~Figure 8~~)**Figure 8**).

As expected, the HEIMS shows better agreement at fday=0 as fire emissions were assimilated on the day. For fday=+1 (i.e. Nov. 12) the HEIMS shows better agreement in RMSE and mean bias (RMSE=58.1 x10^{-6} kg/m^2, bias = -22.4 x10^{-6} kg/m^2 compared with RMSE=63.0 x10^{-6} kg/m^2, bias = -42.2 x10^{-6} kg/m^2) while SFS has better slope. For fday=+2, HEIMS is better in mean bias but worse in RMSE and R. ~~Table 5~~**Table 5** summarizes RMSE statistics from HEIMS and SFS for each day of November 2016. In most of days, HEIMS posts better statistics compared with SFS, implying the potential benefit of system improvement by adding an additional observational constraint. For the comparisons of HEIMS hindcast and SFS operational simulations, HEIMS system shows better performance in both hindcast days (16/19=84% on fday=+1 and 13/19=68% on fday=+2).

Change of fire activity is also a problem for both systems. If there is considerable change of fire activity for fday=+1 & +2, the forecast will result in worse performance. If fire activities increase, the simulated smoke from HEIMS will be underestimated, and if fire activities decrease, the HEIMS system will overestimate the impact of smoke. Therefore, information of next day fire activity, or fire duration, will be important for an accurate fire smoke forecast system, which will be discussed further in the next section.

~~4.6.~~4.6 Persistency of fire activity

The selection of the persistent rate of daily fire emissions (i.e. persistency = 1-decaying_rate) and its importance to the smoke forecast system's performance are discussed here. In our current systems, both SFS and HEIMS, we use a simple assumption of fire emission change for next day. ~~Figure 9~~**Figure 9** shows how the HEIMS responds to the selection of persistent rate for forecast days fday=+1 and +2. We applied five different persistent rates ranging from 0% to 100%; persistency=0% assumes no new fire occurs and persistency=100% assumes the same amount of fire emissions released at

서식 지정함: 글꼴: Times New Roman, 10 pt, 글꼴 색: 자동

서식 있음: 간격 앞: 0 pt

서식 지정함: 글꼴: 굵게

서식 지정함: 글꼴: 굵게

서식 지정함: 글꼴: 굵게

서식 지정함: 글꼴: 굵게

서식 지정함: 글꼴: 굵게

서식 있음: 제목 2, 간격 앞: 0 pt, 글머리 기호 또는 번호 없이

서식 있음: 간격 앞: 0 pt

서식 지정함: 글꼴: 굵게

서식 있음: 가운데

the same location from the previous day. ~~From~~For the top panel of ~~**Figure 9**~~**Figure 9,** simulated smokes in fday=+1 and +2 are sorely originated from fires in fday=0. On the other hand, persistency=100% simulation demonstrates accumulated impacts (target day and previous days), showing denser smokes estimated compared with persistency=0%.

An implication from these comparisons is the importance of persistent rate selection. Indeed, better smoke forecasting may require improvement via two separate steps. The first one is to estimate today's emissions, which can be improved by better assimilation techniques as we introduce in this paper. The second issue is to predict fire activity, which is more related to the studies of fire behavior. In more detail, we need to predict how long existing fires persist, and also to predict the occurrence of new fires, which may pose the greatest difficulty for daily operational systems. Without a better understanding and modeling of fire behavior, the current system has to ~~reply~~rely on the empirical solution. For our case study, choosing persistent rate of 50%/day produced the best result, but it warrants further study with a long-term data set to be used in an operational system. Prediction of wildfire consistency based on the change of meteorological conditions, such as the Fire Weather Index (FWI, ~~https://cwfis.cfs.nrcan.gc.ca/background/summary/fwi),~~https://cwfis.cfs.nrcan.gc.ca/background/summary/fwi), will be a good indicator for the change of fire emission. Without this kind of fire behavior model, the fire smoke forecast system could be limited.

~~5.~~5 Summary and Discussion

Accurate estimation of emissions from wildfire sources is critical to improving the performance of air-quality forecast systems. Wildfire emissions may be estimated based on fire-detection information from the surface (bottom up) or instead based on the intensity of radiance measured from space (top down). This study extends the top-down approach by applying an additional constraint, i.e. transported smoke ~~transport~~plume recorded by geostationary satellites. We developed an inverse modeling system to estimate wildfire smoke emissions over North America using NOAA's HYSPLIT and GOES Aerosol/Smoke products. This HEIMS-fire resolves the strength of smoke sources as a function of time and vertical level. The system adjusts estimated wildfire smoke emissions until they agree well with satellite observations.

We conducted numerous sensitivity tests, varying the temporal, vertical, and spatial coverage of the input data sets used to initiate the inverse system. Results are mostly consistent with general expectations based on the characteristics and behavior of fire events. As transport from previous days can impact large areas, including multiple days of observations to constrain fire emissions yields statistically better results. Including more vertical layers also leads to better results; for example, including the 5000-m layer especially resulted in the best improvement. Spatial coverage was tested in terms of four different domains, and while this particular test presented no solid conclusion, adding more information in general yielded better results, as expected. It also should be noted that the uncertainties of the emission estimation and the smoke forecasts thereafter are not quantified in this study. An ensemble of HYSPLIT predictions using different meteorological inputs will be used to estimate the uncertainties of the results in the future.

서식 있음: 제목 1, 간격 앞: 0 pt, 글머리 기호 또는 번호 없이

서식 있음: 간격 앞: 0 pt

서식 지정함: 글꼴: 굵게 없음

서식 있음: 가운데

For operational purposes, ~~adding a~~including an additional constraint that extends current smoke forecast systems to use smoke plume transport has clear advantages. Future study could improve this approach in several respects. First, the conversion of AOD to smoke mass loading is simply empirical; secondary formation of PM is not considered. Omission of chemical reaction models is the basic characteristic of trajectory- or dispersion-based models compared with Eulerian, full chemistry models. Applying estimated emissions to a chemistry dispersion model could improve results. Second, the system is highly dependent on the quality of constraining observations. Use of the latest satellite instruments could further improve results. Third, we have not yet included surface observations into the inverse system. Utilizing both surface and more columnar observations from other satellite systems will improve the model performance. Fourth, we only used the target day fire emissions for smoke forecast. Since fire smokes last several days, including previous days' emissions will enhance the background effect.

This study aimed to improve the operational smoke forecast by providing accurate fire emission inputs. Unfortunately, the GASP product was discontinued in early 2018. However, the concept of minimizing a cost function based on satellite observations remains robust and can be applied to other data sets. In particular, we plan to apply the GOES-R Advanced Baseline Imager (ABI) product to constrain the extension of fire smoke.

~~6.~~6 References

Ahmadov, R., Grell, G., James, E., Csiszar, I., Tsidulko, M., Pierce, B., McKeen, S., Benjamin, S., Alexander, C., Pereira, G., Freitas, S. and Goldberg, M.: Using VIIRS fire radiative power data to simulate biomass burning emissions, plume rise and smoke transport in a real-time air quality modeling system, in 2017 IEEE International Geoscience and Remote Sensing Symposium (IGARSS), pp. 2806–2808, IEEE., 2017.

Andreae, M. O.: Emission of trace gases and aerosols from biomass burning - An updated assessment, Atmos. Chem. Phys., 19(13), 8523–8546, doi:10.5194/acp-19-8523-2019, 2019.

Arya, S. P.: Air Pollution Meteorology and Dispersion, Oxford University Press., 1998.

Boichu, M., Clarisse, L., Khvorostyanov, D. and Clerbaux, C.: Improving volcanic sulfur dioxide cloud dispersal forecasts by progressive assimilation of satellite observations, Geophys. Res. Lett., 41(7), 2637–2643, doi:10.1002/2014GL059496, 2014.

Bowman, D. M. J. S. D., Balch, J. J. K., Artaxo, P., Bond, W. J., Carlson, J. M., Cochrane, M. A., D'Antonio, C. M., DeFries, R. S., Doyle, J. C., Harrison, S. P., Johnston, F. H., Keeley, J. E., Krawchuk, M. A., Kull, C. A., Marston, J. B., Moritz, M. A., Prentice, I. C., Roos, C. I., Scott, A. C., Swetnam, T. W., Van Der Werf, G. R. and Pyne, S. J.: Fire in the Earth system, Science (80-.)., 324(5926), 481–484, doi:10.1126/science.1163886, 2009.

Briggs, G. A.: Plume rise. Report for U.S. Atomic Energy Commission, Critical Review Series, Technical Information Division report TID-25075, Oak Ridge. [online] Available from: https://www.osti.gov/servlets/purl/4743102, 1969.

Carvalho, A., Monteiro, A., Flannigan, M., Solman, S., Miranda, A. I. I. and Borrego, C.: Forest fires in a changing climate

서식 지정함: 글꼴: 굵게 없음

서식 지정함: 글꼴: 굵게 없음

서식 있음: 제목 1, 간격 앞: 0 pt, 글머리 기호 또는 번호 없이

서식 지정함: 글꼴: +본문(Times New Roman), 굵게 없음

서식 있음: 간격 앞: 0 pt

서식 있음: 간격 앞: 0 pt

서식 있음: 가운데

and their impacts on air quality, Atmos. Environ., 45(31), 5545–5553, doi:10.1016/j.atmosenv.2011.05.010, 2011.

Chai, T., Draxler, R. and Stein, A.: Source term estimation using air concentration measurements and a Lagrangian dispersion model – Experiments with pseudo and real cesium-137 observations from the Fukushima nuclear accident, Atmos. Environ., 106, 241–251, doi:10.1016/j.atmosenv.2015.01.070, 2015.

Chai, T., Crawford, A., Stunder, B., Pavolonis, M. J., Draxler, R. and Stein, A.: Improving volcanic ash predictions with the HYSPLIT dispersion model by assimilating MODIS satellite retrievals, Atmos. Chem. Phys., 17(4), 2865–2879, doi:10.5194/acp-17-2865-2017, 2017.

Chand, D., Guyon, P., Artaxo, P., Schmid, O., Frank, G. P., Rizzo, L. V., Mayol-Bracero, O. L., Gatti, L. V. and Andreae, M. O.: Optical and physical properties of aerosols in the boundary layer and free troposphere over the Amazon Basin during the biomass burning season, Atmos. Chem. Phys., 6(10), 2911–2925, doi:10.5194/acp-6-2911-2006, 2006.

Chen, J., Anderson, K., Pavlovic, R., Moran, M. D., Englefield, P., Thompson, D. K., Munoz-Alpizar, R. and Landry, H.: The FireWork v2.0 air quality forecast system with biomass burning emissions from the Canadian Forest Fire Emissions Prediction System v2.03, Geosci. Model Dev. Discuss., 12(7), 1–41, doi:10.5194/gmd-2019-63, 2019.

Chen, Y., Randerson, J. T., Morton, D. C., DeFries, R. S., Collatz, G. J., Kasibhatla, P. S., Giglio, L., Jin, Y. and Marlier, M. E.: Forecasting Fire Season Severity in South America Using Sea Surface Temperature Anomalies, Science (80-.)., 334(6057), 787–791, doi:10.1126/science.1209472, 2011.

Crawford, A. M., Stunder, B. J. B. B., Ngan, F. and Pavolonis, M. J.: Initializing HYSPLIT with satellite observations of volcanic ash: A case study of the 2008 Kasatochi eruption, J. Geophys. Res. Atmos., 121(18), 10,786-10,803, doi:10.1002/2016JD024779, 2016.

Crutzen, P. J. and Andreae, M. O.: Biomass burning in the tropics: impact on atmospheric chemistry and biogeochemical cycles., Science, 250(4988), 1669–78, doi:10.1126/science.250.4988.1669, 1990.

Draxler, R. R. and Rolph, G. D.: Evaluation of the Transfer Coefficient Matrix (TCM) approach to model the atmospheric radionuclide air concentrations from Fukushima, J. Geophys. Res. Atmos., 117(D5), n/a-n/a, doi:10.1029/2011JD017205, 2012.

Dreessen, J., Sullivan, J. and Delgado, R.: Observations and impacts of transported Canadian wildfire smoke on ozone and aerosol air quality in the Maryland region on June 9–12, 2015, J. Air Waste Manage. Assoc., 66(9), 842–862, doi:10.1080/10962247.2016.1161674, 2016.

Ellicott, E., Vermote, E., Giglio, L. and Roberts, G.: Estimating biomass consumed from fire using MODIS FRE, Geophys. Res. Lett., 36(13), L13401, doi:10.1029/2009GL038581, 2009.

Flannigan, M. D., Logan, K. a., Amiro, B. D., Skinner, W. R. and Stocks, B. J.: Future Area Burned in Canada, Clim. Change, 72(1–2), 1–16, doi:10.1007/s10584-005-5935-y, 2005.

Freeborn, P. H., Wooster, M. J., Roberts, G., Malamud, B. D. and Xu, W.: Development of a virtual active fire product for Africa through a synthesis of geostationary and polar orbiting satellite data, Remote Sens. Environ., 113(8), 1700–1711, doi:10.1016/j.rse.2009.03.013, 2009.

서식 있음: 간격 앞: 0 pt

서식 있음: 간격 앞: 0 pt

서식 있음: 가운데

Giglio, L., Descloitres, J., Justice, C. O. and Kaufman, Y. J.: An enhanced contextual fire detection algorithm for MODIS, Remote Sens. Environ., 87(2–3), 273–282, doi:10.1016/S0034-4257(03)00184-6, 2003.

Green, M., Kondragunta, S., Ciren, P. and Xu, C.: Comparison of GOES and MODIS Aerosol Optical Depth (AOD) to Aerosol Robotic Network (AERONET) AOD and IMPROVE PM 2.5 Mass at Bondville, Illinois, J. Air Waste Manage. Assoc., 59(9), 1082–1091, doi:10.3155/1047-3289.59.9.1082, 2009.

Hobbs, P. V., Reid, J. S., Herring, J. A., Nance, J. D. and Weiss, R. E.: Particle and Trace-Gas Measurements in the Smoke from Prescribed Burns of Forest Products in the Pacific Northwest, in Biomass Burning and Global Change, edited by J. S. Levine, pp. 697–715, MIT Press, New York., 1996.

Ichoku, C. and Ellison, L.: Global top-down smoke-aerosol emissions estimation using satellite fire radiative power measurements, Atmos. Chem. Phys., 14(13), 6643–6667, doi:10.5194/acp-14-6643-2014, 2014.

In, H.-J. J., Byun, D. W., Park, R. J., Moon, N.-K. K., Kim, S. and Zhong, S.: Impact of transboundary transport of carbonaceous aerosols on the regional air quality in the United States: A case study of the South American wildland fire of May 1998, J. Geophys. Res., 112(7), 1–16, doi:10.1029/2006JD007544, 2007.

Jaffe, D. A. and Wigder, N. L.: Ozone production from wildfires: A critical review, Atmos. Environ., 51, 1–10, doi:10.1016/j.atmosenv.2011.11.063, 2012.

Jordan, N. S., Ichoku, C. and Hoff, R. M.: Estimating smoke emissions over the US Southern Great Plains using MODIS fire radiative power and aerosol observations, Atmos. Environ., 42(9), 2007–2022, doi:10.1016/j.atmosenv.2007.12.023, 2008.

Kaiser, J. W., Heil, A., Andreae, M. O., Benedetti, A., Chubarova, N., Jones, L., Morcrette, J.-J. J., Razinger, M., Schultz, M. G., Suttie, M. and van der Werf, G. R.: Biomass burning emissions estimated with a global fire assimilation system based on observed fire radiative power, Biogeosciences, 9(1), 527–554, doi:10.5194/bg-9-527-2012, ~~2012a~~2012.

~~Kaiser, J. W., Heil, A., Andreae, M. O., Benedetti, A., Chubarova, N., Jones, L., Morcrette, J. J., Razinger, M., Schultz, M. G., Suttie, M. and van der Werf, G. R.: Biomass burning emissions estimated with a global fire assimilation system based on observed fire radiative power, Biogeosciences, 9(1), 527–554, doi:10.5194/bg-9-527-2012, 2012b.~~

Katata, G., Chino, M., Kobayashi, T., Terada, H., Ota, M., Nagai, H., Kajino, M., Draxler, R., Hort, M. C., Malo, A., Torii, T. and Sanada, Y.: Detailed source term estimation of the atmospheric release for the Fukushima Daiichi Nuclear Power Station accident by coupling simulations of an atmospheric dispersion model with an improved deposition scheme and oceanic dispersion model, Atmos. Chem. Phys., 15(2), 1029–1070, doi:10.5194/acp-15-1029-2015, 2015.

Kaufman, Y. J., Justice, C. O., Flynn, L. P., Kendall, J. D., Prins, E. M., Giglio, L., Ward, D. E., Menzel, W. P. and Setzer, A. W.: Potential global fire monitoring from EOS-MODIS, J. Geophys. Res. Atmos., 103(D24), 32215–32238, doi:10.1029/98JD01644, 1998.

Kondragunta, S., Lee, P., McQueen, J., Kittaka, C., Prados, ~~a~~A. I., Ciren, P., Laszlo, I., Pierce, R. B., Hoff, R. and Szykman, J. J.: Air Quality Forecast Verification Using Satellite Data, J. Appl. Meteorol. Climatol., 47(2), 425–442, doi:10.1175/2007JAMC1392.1, 2008.

Kunik, L., Mallia, D. V., Gurney, K. R., Mendoza, D. L., Oda, T. and Lin, J. C.: Bayesian inverse estimation of urban CO2

서식 있음: 간격 앞: 0 pt

서식 있음: 간격 앞: 0 pt

서식 있음: 가운데

emissions: Results from a synthetic data simulation over Salt Lake City, UT, Elem Sci Anth, 7(1), 36, doi:10.1525/elementa.375, 2019.

Larkin, N. K., O'Neill, S. M., Solomon, R., Raffuse, S., Strand, T., Sullivan, D. C., Krull, C., Rorig, M., Peterson, J. and Ferguson, S. A.: The BlueSky smoke modeling framework, Int. J. Wildl. Fire, 18(8), 906, doi:10.1071/WF07086, 2009.

Lee, B., Cho, S., Lee, S.-K., Woo, C. and Park, J.: Development of a Smoke Dispersion Forecast System for Korean Forest Fires, Forests, 10(3), 219, doi:10.3390/f10030219, 2019.

Lee, P., McQueen, J., Stajner, I., Huang, J., Pan, L., Tong, D., Kim, H., Tang, Y., Kondragunta, S., Ruminski, M., Lu, S., Rogers, E., Saylor, R., Shafran, P., Huang, H.-C., Gorline, J., Upadhayay, S. and Artz, R.: NAQFC Developmental Forecast Guidance for Fine Particulate Matter (PM 2.5), Weather Forecast., 32(1), 343–360, doi:10.1175/WAF-D-15-0163.1, 2017.

Li, X., Sun, S., Hu, X., Huang, H., Li, H., Morino, Y., Wang, S., Yang, X., Shi, J. and Fang, S.: Source inversion of both long- and short-lived radionuclide releases from the Fukushima Daiichi nuclear accident using on-site gamma dose rates, J. Hazard. Mater., 379, 120770, doi:10.1016/j.jhazmat.2019.120770, 2019a.

Li, Y., Liu, J., Han, H., Zhao, T., Zhang, X., Zhuang, B., Wang, T., Chen, H., Wu, Y. and Li, M.: Collective impacts of biomass burning and synoptic weather on surface PM2.5 and CO in Northeast China, Atmos. Environ., 213, 64–80, doi:10.1016/j.atmosenv.2019.05.062, ~~2019~~2019b.

Liu, Y., Goodrick, S. and Heilman, W.: Wildland fire emissions, carbon, and climate: Wildfire-climate interactions, For. Ecol. Manage., 317, 80–96, doi:10.1016/j.foreco.2013.02.020, 2014.

Mok, J., Krotkov, N. A., Arola, A., Torres, O., Jethva, H., Andrade, M., Labow, G., Eck, T. F., Li, Z., Dickerson, R. R., Stenchikov, G. L., Osipov, S. and Ren, X.: Impacts of brown carbon from biomass burning on surface UV and ozone photochemistry in the Amazon Basin, Sci. Rep., 6(1), 36940, doi:10.1038/srep36940, 2016.

Nickless, A., Rayner, P. J., Engelbrecht, F., Brunke, E.-G., Erni, B. and Scholes, R. J.: Estimates of CO 2 fluxes over the city of Cape Town, South Africa, through Bayesian inverse modelling, Atmos. Chem. Phys., 18(7), 4765–4801, doi:10.5194/acp-18-4765-2018, 2018.

Nikonovas, T., North, P. R. J. and Doerr, S. H.: Particulate emissions from large North American wildfires estimated using a new top-down method, Atmos. Chem. Phys., 17(10), 6423–6438, doi:10.5194/acp-17-6423-2017, 2017.

Paciorek, C. J., Liu, Y., Moreno-Macias, H. and Kondragunta, S.: Spatiotemporal Associations between GOES Aerosol Optical Depth Retrievals and Ground-Level PM 2.5, Environ. Sci. Technol., 42(15), 5800–5806, doi:10.1021/es703181j, 2008.

Pan, X., Ichoku, C., Chin, M., Bian, H., Darmenov, A., Colarco, P., Ellison, L., Kucsera, T., da Silva, A., Wang, J., Oda, T. and Cui, G.: Six global biomass burning emission datasets: intercomparison and application in one global aerosol model, Atmos. Chem. Phys., 20(2), 969–994, doi:10.5194/acp-20-969-2020, 2020.

Pavlovic, R., Chen, J., Anderson, K., Moran, M. D., Beaulieu, P.-A., Davignon, D. and Cousineau, S.: The FireWork air quality forecast system with near-real-time biomass burning emissions: Recent developments and evaluation of performance for the 2015 North American wildfire season, J. Air Waste Manage. Assoc., 66(9), 819–841,

서식 있음: 간격 앞: 0 pt

서식 있음: 간격 앞: 0 pt

서식 있음: 간격 앞: 0 pt

서식 있음: 간격 앞: 0 pt

서식 있음: 가운데

doi:10.1080/10962247.2016.1158214, 2016.

Prados, A. I., Kondragunta, S., Ciren, P. and Knapp, K. R.: GOES Aerosol/Smoke Product (GASP) over North America: Comparisons to AERONET and MODIS observations, J. Geophys. Res., 112(D15), D15201, doi:10.1029/2006JD007968, 2007.

Reid, J. S., Eck, T. F., Christopher, S. A., Koppmann, R., Dubovik, O., Eleuterio, D. P., Holben, B. N., Reid, E. A. and Zhang, J.: A review of biomass burning emissions part III: intensive optical properties of biomass burning particles, Atmos. Chem. Phys., 5(3), 827–849, doi:10.5194/acp-5-827-2005, 2005.

Rolph, G. D., Draxler, R. R., Stein, A. F., Taylor, A., Ruminski, M. G., Kondragunta, S., Zeng, J., Huang, H.-C. C., Manikin, G., McQueen, J. T. and Davidson, P. M.: Description and verification of the NOAA smoke forecasting system: The 2007 fire season, Weather Forecast., 24(2), 361–378, doi:10.1175/2008WAF2222165.1, 2009.

Ruminski, M. and Kondragunta, S.: Monitoring fire and smoke emissions with the hazard mapping system, in Disaster Forewarning Diagnostic Methods and Management, vol. 6412, edited by F. Kogan, S. Habib, V. S. Hegde, and M. Matsuoka, p. 64120B., 2006.

Ruminski, M., Simko, J., Kibler, J., Kondragunta, S., Draxler, R., Davidson, P. and Li, P.: Use of multiple satellite sensors in NOAA's operational near real-time fire and smoke detection and characterization program, in Remote Sensing of Fire: Science and Application, vol. 7089, edited by W. M. Hao, p. 70890A., 2008.

Schroeder, W., Ruminski, M., Csiszar, I., Giglio, L., Prins, E., Schmidt, C. and Morisette, J.: Validation analyses of an operational fire monitoring product: The Hazard Mapping System, Int. J. Remote Sens., 29(20), 6059–6066, doi:10.1080/01431160802235845, 2008.

Schroeder, W., Ellicott, E., Ichoku, C., Ellison, L., Dickinson, M. B., Ottmar, R. D., Clements, C., Hall, D., Ambrosia, V. and Kremens, R.: Integrated active fire retrievals and biomass burning emissions using complementary near-coincident ground, airborne and spaceborne sensor data, Remote Sens. Environ., 140, 719–730, doi:10.1016/j.rse.2013.10.010, 2014.

Seiler, W. and Crutzen, P. J.: Estimates of gross and net fluxes of carbon between the biosphere and the atmosphere from biomass burning, Clim. Change, 2(3), 207–247, doi:10.1007/BF00137988, 1980.

Singh, H. B. B., Cai, C., Kaduwela, A., Weinheimer, A. a. and Wisthaler, A. a.: Interactions of fire emissions and urban pollution over California: Ozone formation and air quality simulations, Atmos. Environ., 56, 45–51, doi:10.1016/j.atmosenv.2012.03.046, 2012.

Sofiev, M., Vankevich, R., Lotjonen, M., Prank, M., Petukhov, V., Ermakova, T., Koskinen, J. and Kukkonen, J.: An operational system for the assimilation of the satellite information on wild-land fires for the needs of air quality modelling and forecasting, Atmos. Chem. Phys., 9(18), 6833–6847, doi:10.5194/acp-9-6833-2009, 2009.

Spracklen, D. V., Mickley, L. J., Logan, J. a., Hudman, R. C., Yevich, R., Flannigan, M. D. and Westerling, a. L.: Impacts of climate change from 2000 to 2050 on wildfire activity and carbonaceous aerosol concentrations in the western United States, J. Geophys. Res., 114(D20), D20301, doi:10.1029/2008JD010966, 2009.

Stein, a. F., Draxler, R. R., Rolph, G. D., Stunder, B. J. B. B., Cohen, M. D. and Ngan, F.: NOAA's HYSPLIT Atmospheric

서식 있음: 간격 앞: 0 pt

서식 있음: 가운데

Transport and Dispersion Modeling System, Bull. Am. Meteorol. Soc., 96(12), 2059–2077, doi:10.1175/BAMS-D-14-00110.1, 2015.

Stein, A. F., Rolph, G. D., Draxler, R. R., Stunder, B. and Ruminski, M.: Verification of the NOAA Smoke Forecasting System: Model Sensitivity to the Injection Height, Weather Forecast., 24(2), 379–394, doi:10.1175/2008WAF2222166.1, 2009.

Strand, T. M., Larkin, N., Craig, K. J., Raffuse, S., Sullivan, D., Solomon, R., Rorig, M., Wheeler, N. and Pryden, D.: Analyses of BlueSky Gateway PM 2.5 predictions during the 2007 southern and 2008 northern California fires, J. Geophys. Res. Atmos., 117(D17), n/a-n/a, doi:10.1029/2012JD017627, 2012.

Turnbull, J. C., Karion, A., Davis, K. J., Lauvaux, T., Miles, N. L., Richardson, S. J., Sweeney, C., McKain, K., Lehman, S. J., Gurney, K. R., Patarasuk, R., Liang, J., Shepson, P. B., Heimburger, A., Harvey, R. and Whetstone, J.: Synthesis of Urban CO 2 Emission Estimates from Multiple Methods from the Indianapolis Flux Project (INFLUX), Environ. Sci. Technol., 53(1), 287–295, doi:10.1021/acs.est.8b05552, 2019.

Val Martin, M., Logan, J. A., Kahn, R. A., Leung, F.-Y. Y., Nelson, D. L. and Diner, D. J.: Smoke injection heights from fires in North America: Analysis of 5 years of satellite observations, Atmos. Chem. Phys., 10(4), 1491–1510, doi:10.5194/acp-10-1491-2010, 2010.

Valerino, M. J., Johnson, J. J., Izumi, J., Orozco, D., Hoff, R. M., Delgado, R. and Hennigan, C. J.: Sources and composition of PM 2.5 in the Colorado Front Range during the DISCOVER-AQ study, J. Geophys. Res. Atmos., 122(1), 566–582, doi:10.1002/2016JD025830, 2017.

Vermote, E., Ellicott, E., Dubovik, O., Lapyonok, T., Chin, M., Giglio, L. and Roberts, G. J.: An approach to estimate global biomass burning emissions of organic and black carbon from MODIS fire radiative power, J. Geophys. Res., 114(D18), 1–22, doi:10.1029/2008JD011188, 2009.

van der Werf, G. R., Randerson, J. T., Giglio, L., Collatz, G. J., Mu, M., Kasibhatla, P. S., Morton, D. C., DeFries, R. S., Jin, Y. and van Leeuwen, T. T.: Global fire emissions and the contribution of deforestation, savanna, forest, agricultural, and peat fires (1997–2009), Atmos. Chem. Phys., 10(23), 11707–11735, doi:10.5194/acp-10-11707-2010, 2010.

Wiedinmyer, C., Quayle, B., Geron, C., Belote, A., McKenzie, D., Zhang, X., O'Neill, S., Wynne, K. K., O'Neill, S. and Wynne, K. K.: Estimating emissions from fires in North America for air quality modeling, Atmos. Environ., 40(19), 3419–3432, doi:10.1016/j.atmosenv.2006.02.010, 2006.

Wiedinmyer, C., Akagi, S. K., Yokelson, R. J., Emmons, L. K., Al-Saadi, J. A., Orlando, J. J. and Soja, ~~A~~ a. J.: The Fire INventory from NCAR (FINN): a high resolution global model to estimate the emissions from open burning, Geosci. Model Dev., 4(3), 625–641, doi:10.5194/gmd-4-625-2011, 2011.

Zhang, X., Kondragunta, S., Ram, J., Schmidt, C. and Huang, H.-C.: Near-real-time global biomass burning emissions product from geostationary satellite constellation, J. Geophys. Res. Atmos., 117(D14), n/a-n/a, doi:10.1029/2012JD017459, 2012.

Zhu, C., Byrd, R. H., Lu, P. and Nocedal, J.: Algorithm 778: L-BFGS-B: Fortran subroutines for large-scale bound-

서식 있음: 간격 앞: 0 pt

서식 있음: 가운데

constrained optimization, ACM Trans. Math. Softw., 23(4), 550–560, doi:10.1145/279232.279236, 1997.

Zidikheri, M. J. and Lucas, C.: Using Satellite Data to Determine Empirical Relationships between Volcanic Ash Source Parameters, Atmosphere (Basel)., 11(4), 342, doi:10.3390/atmos11040342, 2020.

서식 있음: 간격 앞: 0 pt

서식 있음: 가운데

630


Copernicus Publications
The Innovative Open Access Publisher

서식 있음: 가운데

635 **Table 1. Performance evaluation. Statistics of modeled smoke mass loading ($x10^{-6}$ kg/m^2) using initial and top-down estimated fire emissions.**

		Nov. 10	Nov. 11	Nov. 12	Nov. 13	Nov. 14	Nov. 15	Nov. 16	Nov. 17
mean	Observation	42.4884.95	52.67105.34	74.35148.71	79.90159.67	94.20188.40	92.29184.57	63.68127.36	50.70101.41
	Initial	18.7237.53	18.2236.44	7.8815.75	17.2534.51	14.8129.61	9.4818.96	4.639.26	3.416.83
	Inverse	73.72	77.92	108.20	105.24	122.15	114.85	87.76	66.14
RMSE	Initial	86.09	99.56	153.21	153.35	184.74	188.81	136.79	104.80
	Inverse	36.8654.07	38.9669.37	54.1094.40	52.62104.85	61.08124.88	57.42130.89	43.8892.35	33.0770.77
RMSENRMSE [%]	Initial	43.05101.34	49.7894.51	76.60103.02	76.6896.01	92.3798.06	94.40102.30	68107.40	52.40103.34
	Inverse	27.0463.64	34.6965.85	47.2063.48	52.4365.67	62.4466.28	65.4570.92	46.1872.51	35.3969.79
Slope	Initial	0.88	0.74	0.33	0.54	0.46	0.24	-0.15	0.26
	Inverse	0.73	0.89	0.99	1.07	1.07	1.07	0.89	1.14
R	Initial	0.4	0.46	0.02	0.18	0.28	0.25	-0.08	0.00
	Inverse	0.65	0.62	0.31	0.48	0.44	0.35	0.15	0.15

640

서식 있음: 가운데

Table 2. Sensitivity test for temporal coverage. Uses of ~~observational data~~assimilation (A), observation (O), and evaluation (E) time windows (24 hours to 96 hours) were tested, and statistics, ~~RMSE~~NRMSE, and R, were compared. The best performance is marked as bold. ~~[RMSE Unit: 10^{-6} kg/m^2]~~

	~~RMSE~~ NRMSE [%]				R			
Coverage	~~24 hour (oday=0)~~ A: 24h O: 24h E: 24h	~~48 hour (oday=-1)~~A: 48h O: 48h E: 48h	~~72 hour (oday=-2)~~A: 72h O: 72h E: 72h	~~96 hour (oday=-3)~~A: 96h O: 96h E: 96h	~~24 hour (oday=0)~~ A: 24h O: 24h E: 24h	~~48 hour (oday=-1)~~A: 48h O: 48h E: 48h	~~72 hour (oday=-2)~~A: 72h O: 72h E: 72h	~~96 hour (oday=-3)~~A: 96h O: 96h E: 96h
Nov. 10 11 12 13 14 15 16 17	~~**24.97**~~ ~~58.28~~ ~~51.93~~ ~~64.74~~ ~~80.76~~ ~~70.04~~ ~~**35.39**~~ 66.6 75.2 75.1 72.8 75.6 82.7 69.8	~~27.04~~ ~~34.69~~ ~~47.20~~ ~~52.43~~ ~~62.44~~ 63.7 65.~~45~~9 ~~46.18~~ ~~**35.39**~~63.5 65.7 66.3 70.9 72.5 69.8	~~26.~~**62**.7 ~~34.57~~ ~~36.47~~ ~~47.54~~ ~~53.08~~ ~~56.48~~ ~~50.50~~ ~~46.17~~64.0 61.4 59.9 61.0 62.7 68.2 72.5	~~36.98~~ ~~**34.40**~~ ~~**36.33**~~ ~~**38.96**~~ ~~**48.17**~~ ~~**51.88**~~ ~~47.25~~ ~~50.50~~68.7 **63.7** **60.6** **59.6** **56.8** **60.2** **61.7** **68.2**	**0.~~68~~677** 0.~~41~~410 0.~~37~~373 0.~~30~~298 0.~~29~~285 0.~~11~~105 0.~~15~~146	0.~~65~~654 **0.~~62~~620** 0.~~31~~309 0.~~48~~476 0.~~44~~444 0.~~35~~348 0.~~15~~150 0.~~15~~146	0.~~67~~669 0.~~59~~587 **0.~~56~~562** 0.~~40~~397 **0.~~52~~522** 0.~~47~~465 0.~~37~~372 0.~~15~~150	0.~~58~~577 0.~~59~~593 0.~~53~~526 **0.~~58~~576** 0.~~47~~469 **0.~~51~~511** **0.~~48~~478** **0.~~37~~372**
Coverage	A: 24h O: 24h E: 24h	A: 48h O: 48h E: 24h	A: 72h O: 72h E: 24h	A: 96h O: 96h E: 24h	A: 24h O: 24h E: 24h	A: 48h O: 48h E: 24h	A: 72h O: 72h E: 24h	A: 96h O: 96h E: 24h
Nov. 10	66.6	49.1	49.0	**38.7**	0.677	0.713	0.716	**0.716**
11	75.2	80.6	78.4	**78.4**	0.410	0.621	0.623	**0.623**
12	75.1	**45.2**	56.5	55.8	0.373	0.406	0.425	**0.430**
13	72.8	58.0	**52.9**	63.5	0.298	0.534	0.581	**0.589**
14	75.6	54.6	53.8	**53.1**	0.285	0.567	0.593	**0.609**
15	82.7	43.9	**42.4**	44.6	0.105	0.554	**0.589**	0.571
16	69.8	34.3	28.4	**27.4**	0.146	0.464	**0.507**	0.505
17								
Coverage	A: 96h O: 24h E: 24h	A: 96h O: 48h E: 48h	A: 96h O: 72h E: 72h	A: 96h O: 96h E: 96h	A: 96h O: 24h E: 24h	A: 96h O: 48h E: 48h	A: 96h O: 72h E: 72h	A: 96h O: 96h E: 96h
Nov. 10	**53.0**	62.1	62.1	68.7	**0.746**	0.657	0.657	0.577
11	**54.7**	61.9	63.7	63.7	0.583	**0.615**	0.593	0.593
12	**43.0**	54.0	59.1	60.6	0.425	0.481	**0.545**	0.526
13	**40.3**	46.4	54.5	59.6	**0.664**	0.510	0.500	0.576
14	**38.3**	43.5	50.5	56.8	**0.688**	0.603	0.499	0.469
15	**43.9**	50.8	55.3	60.2	**0.647**	0.572	0.533	0.511
16	**33.5**	42.2	53.2	61.7 68.2	0.667	**0.685**	0.581	0.478
17		36.1	53.8			**0.624**	0.520	0.372
Coverage	A: 96h O: 24h E: 24h	A: 96h O: 48h E: 24h	A: 96h O: 72h E: 24h	A: 96h O: 96h E: 24h	A: 96h O: 24h E: 24h	A: 96h O: 48h E: 24h	A: 96h O: 72h E: 24h	A: 96h O: 96h E: 24h
Nov. 10	53.6	47.1	47.1	**38.7**	**0.746**	0.715	0.715	0.716
11	**58.1**	81.0	78.4	78.4	**0.668**	0.624	0.623	0.623

12	**41.3**	48.0	56.7	55.8	**0.489**	0.432	0.433	0.430
13	**39.5**	49.8	55.4	63.5	**0.691**	0.612	0.588	0.589
14	**39.5**	45.8	51.9	53.1	**0.698**	0.612	0.612	0.609
15	**37.8**	43.1	43.1	44.6	**0.682**	0.552	0.566	0.571
16	**33.7**	29.6	27.9	27.4	**0.614**	0.542	0.510	0.505
17								

서식 있음: 가운데

서식 있음: 가운데

Table 3. Sensitivity tests for selection of two to seven layers among 100, 500, 1000, 1500, 2000, 5000, and 10000 meters. Beginning from two layers at 100 and 500 meters, the next higher layer is added for each test. The best performance is marked as bold. ~~[RMSE unit: 10^{-6} kg/m^2]~~

	Date	2 layers (100,500m)	3 layers (100-1000m)	4 layers (100-1500m)	5 layers (100-2000m)	6 layers (100-5000m)	7 layers (100-10000m)
~~RMSE~~NRMSE [%]	Nov. 10	~~31.43~~ ~~44.36~~ ~~50.23~~ ~~61.67~~ ~~77.17~~ ~~75.10~~ ~~51.17~~ ~~36.31~~74.1 82.2 68.6 76.0 78.1 81.1 84.6 81.3	~~29.64~~ ~~40.32~~ ~~48.38~~ ~~59.24~~ 69.9 75.~~96~~6 ~~69.98~~ ~~50.02~~ ~~35.51~~ 65.6 73.2 77.1 75.4 80.8 78.3	~~27.87~~ ~~37.25~~ ~~49.90~~ ~~58.79~~ ~~74.62~~ 65.7 70.1 67.~~79~~0 ~~47.35~~ ~~33.42~~72.8 76.3 73.2 76.4 73.5	~~27.38~~ ~~36.05~~ ~~51.87~~ ~~58.58~~ 64.5 68.4 68.9 72.~~56~~8 ~~65.99~~ ~~45.64~~ ~~34.29~~75.5 71.4 73.7 73.2	~~27.04~~ ~~34.69~~ ~~47.20~~ ~~52.43~~ ~~62.44~~ **63.7** **65.4~~5~~9** ~~46.18~~ ~~35.39~~**63.5** 65.7 **66.3** **70.9** 72.5 **69.8**	~~27.05~~ ~~34.70~~ ~~47.23~~ ~~52.11~~ ~~62.47~~ 63.7 65.4~~5~~9 ~~46.17~~ ~~35.39~~ 63.5 **65.3** 66.3 70.9 **72.5** 69.8
R	Nov. 10	0.58	0.62	0.64	0.65	**0.65**	**0.65**
	11	0.49	0.55	0.60	0.61	0.62	**0.62**
	12	0.23	0.21	0.15	0.12	**0.31**	0.31
	13	0.43	0.44	0.43	0.43	**0.48**	0.47
	14	0.43	0.41	0.41	0.43	**0.44**	**0.44**
	15	0.30	0.34	0.34	**0.35**	0.35	0.35
	16	0.11	0.10	0.12	0.15	0.15	**0.15**
	17	**0.40**	0.34	0.33	0.24	0.15	0.15

서식 지정함: 글꼴: 9 pt

서식 있는 표

서식 지정함: 글꼴: 굵게

서식 있음: 가운데

Table 4. Sensitivity tests for spatial coverage. Use of observational data in terms of spatial availability is tested. Domains 1-4 are shown in ~~Figure 3.~~Figure 3. The best performance is marked as bold. ~~[RMSE unit: 10^{-6}kg/m^2]~~

	Date	Domain 1	Domain 2	Domain 3	Domain 4
		~~51.40~~	~~28.73~~	~~28.51~~	~~**27.04**~~
		~~51.40~~	~~**33.09**~~	~~34.88~~	~~34.69~~
		~~44.37~~	~~**44.25**~~	~~44.45~~	~~47.20~~
	Nov. 10	~~48.04~~	~~48.02~~	~~**48.01**~~	~~52.43~~
	11	~~58.39~~	65.9	~~**58.39**~~	~~62.44~~
	12	64.5	**62.3**	65.7	**63.7**
~~RMSE~~NRMSE	13	64.5	**59.**~~565~~	65.3	65.~~459~~
[%]	14	59.~~557~~	~~***59.48***~~	59.~~568~~	~~46.18~~
	15	~~59.55~~	~~46.06~~	~~**46.01**~~	~~**35.39**~~63.5
	16	~~59.55~~60.1	~~46.06~~ 60.1	~~46.01~~**60.1**	65.7
	17	62.3	63.6	**62.3**	66.3
		66.5	**66.4**	66.5	70.9
		66.5	72.7	72.6	72.5
		66.5	72.7	72.6	69.8
	Nov. 10	0.48	0.62	0.62	**0.65**
	11	0.48	**0.63**	0.62	0.62
	12	**0.32**	0.32	0.31	0.31
R	13	0.47	0.47	0.47	**0.48**
	14	0.43	0.42	0.43	**0.44**
	15	0.33	0.33	0.32	**0.35**
	16	**0.33**	0.15	0.15	0.15
	17	**0.33**	0.15	0.15	0.15

서식 지정함: 글꼴: 9 pt

서식 지정함: 글꼴: 9 pt

서식 있는 표

서식 지정함: 글꼴: 굵게

서식 지정함: 글꼴: 굵게

서식 지정함: 글꼴: 굵게

서식 있음: 가운데

Table 5. Performance statistics, RMSEs, for HEIMS and SFS smoke mass loading for 0-2 forecast days (e.g., fday=0,+1,+2). For each forecast day, the better performance from two systems is marked as bold. ~~Empty statistics are either~~Statistics for days without observations or without operational outputs are available. [Unit: 10^{-6} kg/m^2]

	fday = 0		fday = +1		fday = +2	
Date	HEIMS	SFS	HEIMS	SFS	HEIMS	SFS
November 1	**64.5**	105.8	**54.6**	70.5	**40.2**	77.0
2	**53.6**	70.6	**52.0**	76.2	**51.8**	53.9
3	**61.4**	76.4	**52.8**	54.5	**74.3**	74.4
4	**45.1**	53.3	**67.2**	71.6	106.8	**86.5**
5	**41.6**	70.4	**64.3**	82.4	**68.5**	72.2
6	**54.2**	86.1	**61.6**	95.7	-	-
7	**56.3**	88.3	-	-	75.2	**72.9**
8	-	-	74.8	-	45.0	-
9	**60.4**	73.3	**39.7**	40.3	**69.3**	70.5
10	**22.8**	57.0	61.2	**60.1**	**71.8**	89.1
11	**45.5**	60.3	**58.1**	63.0	95.4	**71.0**
12	**39.9**	60.7	103.0	**69.1**	**79.4**	88.1
13	**52.7**	74.3	**69.7**	83.8	75.3	**61.4**
14	**60.3**	81.9	**61.8**	63.9	**42.0**	44.2
15	57.8	-	31.4	-	-	-
16	**26.6**	39.8	-	-	-	-
17	-	-	-	-	**46.2**	47.0
18	-	-	52.3	**45.6**	45.0	**43.6**
19	**35.6**	49.7	**44.4**	45.8	**42.3**	46.0
20	42.8	-	41.3	-	77.3	-
21	**35.0**	45.2	**64.5**	77.0	**63.7**	76.6
22	49.2	-	54.3	-	43.2	-
23	**60.7**	75.5	**42.7**	46.2	92.7	**92.4**
24	**39.8**	50.9	**89.8**	93.3	**70.4**	71.1
25	**87.6**	93.4	**71.7**	72.1	102.1	**101.6**
26	**62.3**	72.0	**90.6**	100.8	-	-
27	**73.1**	99.8	-	-	-	-
28	-	-	-	-	-	-
29	-	-	-	-	-	-
30	-	-	-	-	**40.0**	40.0
HEIMS Performance	21/21=100%		16/19=84%		13/19=68%	

서식 지정함: 글꼴: 9 pt

서식 지정함: 글꼴: 9 pt

서식 지정함: 글꼴: 9 pt

서식 있는 표

서식 있음: 가운데

서식 있음: 가운데

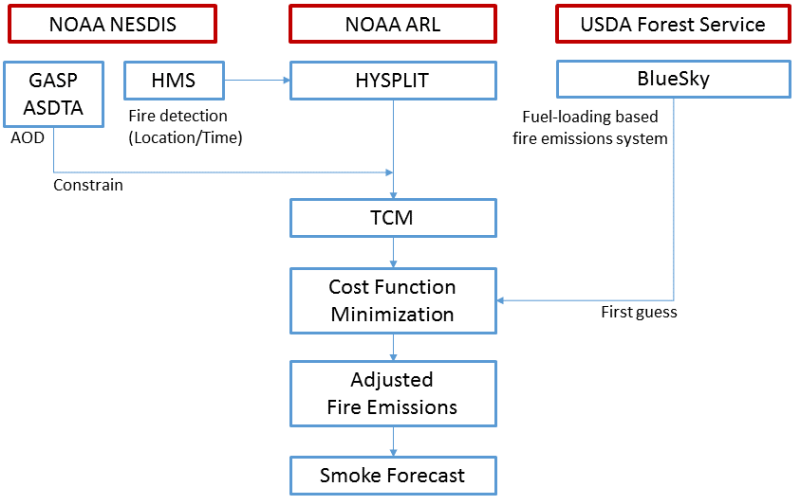

Figure 1. Schematic diagram of the HYSPLIT-based Fire Emission Inverse Modeling System.

서식 지정함: 영어(미국)

서식 지정함: 글꼴: 9 pt

서식 있음: 간격 앞: 0 pt

서식 있음: 가운데

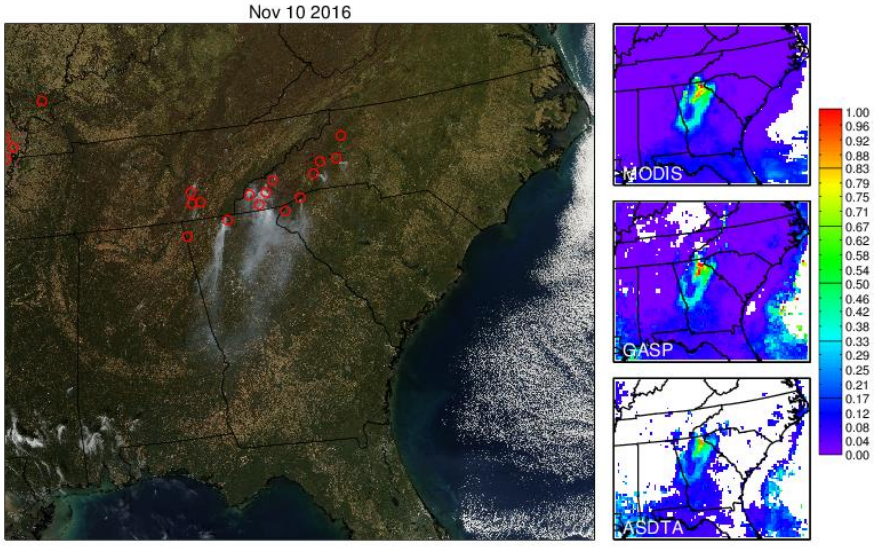

Figure 2. Detection of fires over the southeastern region of the United States on November 10, 2016. ~~True-color~~Truecolor image from MODIS (left), MODIS AOD (top right), GASP AOD (middle right), and ASDTA AOD (bottom right) are shown. MODIS truecolor images and AOD are obtained from earthdata.nasa.gov, and GASP and ASDTA AOD are obtained from NOAA NESDIS.

675

서식 지정함: 영어(미국)

서식 지정함: 글꼴: 9 pt

서식 있음: 간격 앞: 0 pt

서식 지정함: 글꼴: 9 pt

서식 지정함: 글꼴: 9 pt

서식 있음: 가운데

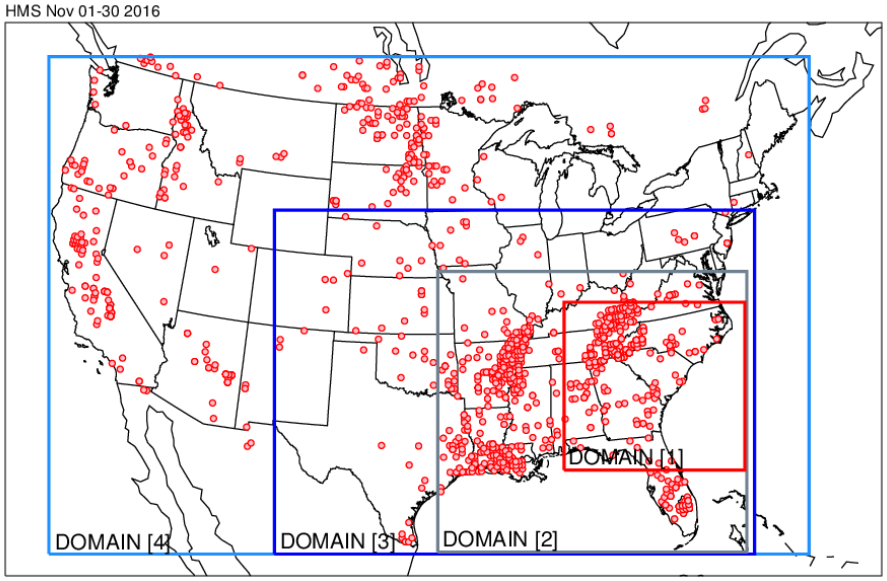

Figure 3. Geographical coverage of case study domains. Red dots indicate HMS fire detections during November 2016. The four labeled domains indicate spatial coverage of fire source inputs for the inverse system used in the sensitivity tests.

서식 지정함: 영어(미국)

서식 지정함: 글꼴: 9 pt

서식 있음: 가운데

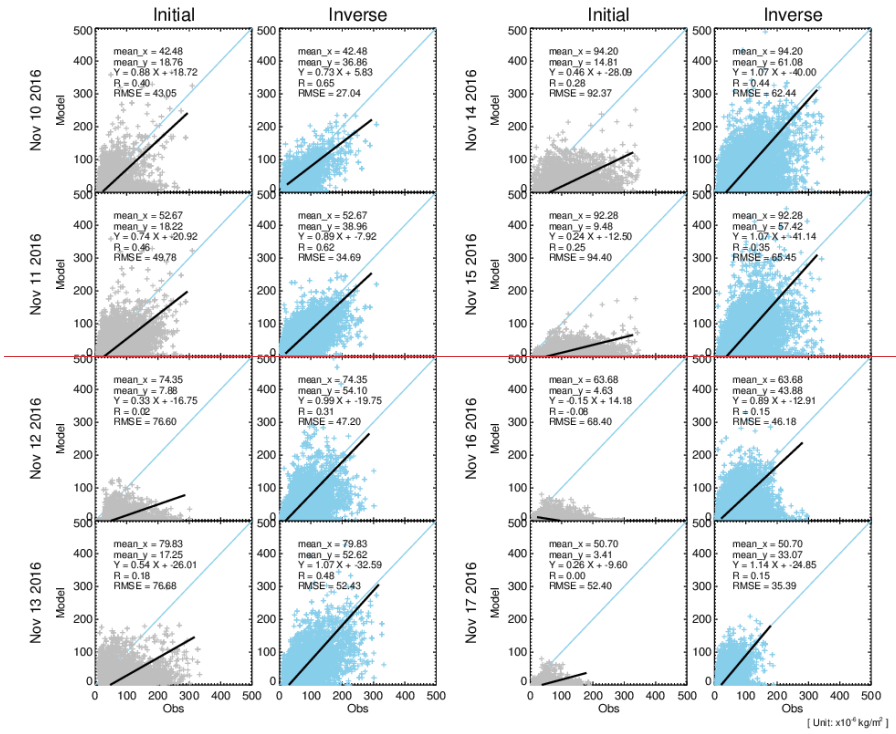
Initial
Inverse
Nov 10 2016
Nov 11 2016
Nov 12 2016
Nov 13 2016
Nov 14 2016
Nov 15 2016
Nov 16 2016
Nov 17 2016
Model
Obs
mean_x = 42.48
mean_y = 18.76
Y = 0.88 X + +18.72
R = 0.40
RMSE = 43.05
mean_x = 42.48
mean_y = 36.86
Y = 0.73 X + 5.83
R = 0.65
RMSE = 27.04
mean_x = 52.67
mean_y = 18.22
Y = 0.74 X + -20.92
R = 0.46
RMSE = 49.78
mean_x = 52.67
mean_y = 38.96
Y = 0.89 X + -7.92
R = 0.62
RMSE = 34.69
mean_x = 74.35
mean_y = 7.88
Y = 0.33 X + -16.75
R = 0.02
RMSE = 76.60
mean_x = 74.35
mean_y = 54.10
Y = 0.99 X + -19.75
R = 0.31
RMSE = 47.20
mean_x = 79.83
mean_y = 17.25
Y = 0.54 X + -26.01
R = 0.18
RMSE = 76.68
mean_x = 79.83
mean_y = 52.62
Y = 1.07 X + -32.59
R = 0.48
RMSE = 52.43
mean_x = 94.20
mean_y = 14.81
Y = 0.46 X + -28.09
R = 0.28
RMSE = 92.37
mean_x = 94.20
mean_y = 61.08
Y = 1.07 X + -40.00
R = 0.44
RMSE = 62.44
mean_x = 92.28
mean_y = 9.48
Y = 0.24 X + -12.50
R = 0.25
RMSE = 94.40
mean_x = 92.28
mean_y = 57.42
Y = 1.07 X + -41.14
R = 0.35
RMSE = 65.45
mean_x = 63.68
mean_y = 4.63
Y = -0.15 X + 14.18
R = -0.08
RMSE = 68.40
mean_x = 63.68
mean_y = 43.88
Y = 0.89 X + -12.91
R = 0.15
RMSE = 46.18
mean_x = 50.70
mean_y = 3.41
Y = 0.26 X + -9.60
R = 0.00
RMSE = 52.40
mean_x = 50.70
mean_y = 33.07
Y = 1.14 X + -24.85
R = 0.15
RMSE = 35.39
[Unit: x10^6 kg/m^2]

서식 있음: 가운데

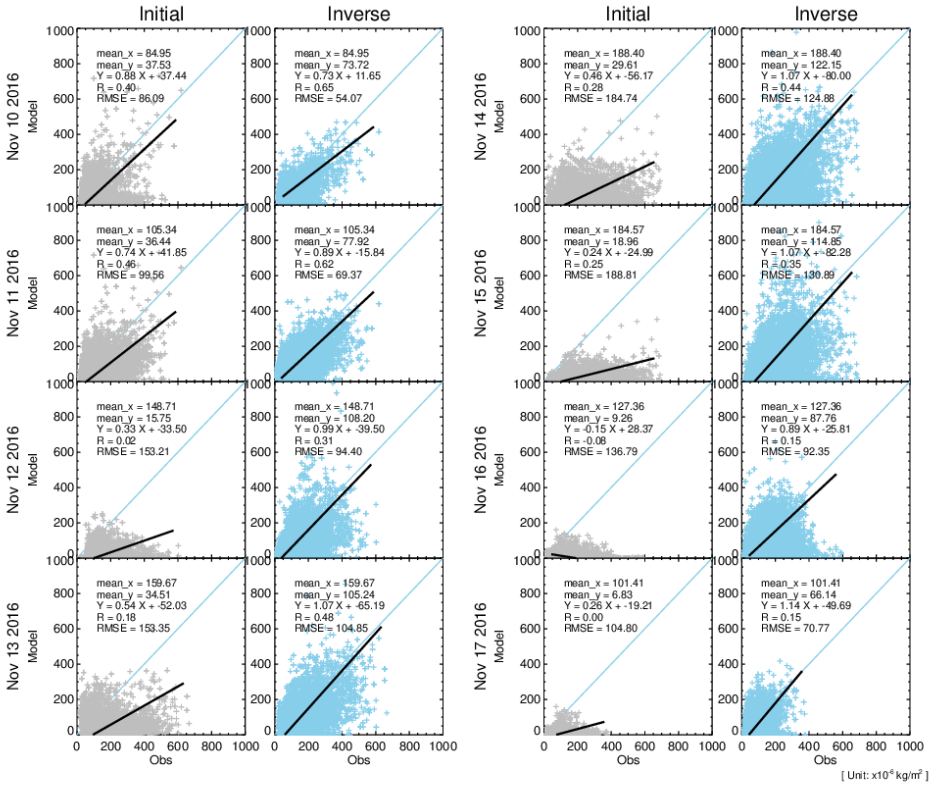

685 **Figure 4. Scatter plot comparison between initial and assimilated smoke mass loading using adjusted fire emissions. A 48-hour observation (~~oday~~aday=-1) and 6-layer plume release configuration is used. [Unit: x10^{-6}kg/m^2]**

서식 지정함: 글꼴: 9 pt

서식 있음: 간격 앞: 0 pt

서식 지정함: 글꼴: 9 pt

서식 있음: 가운데

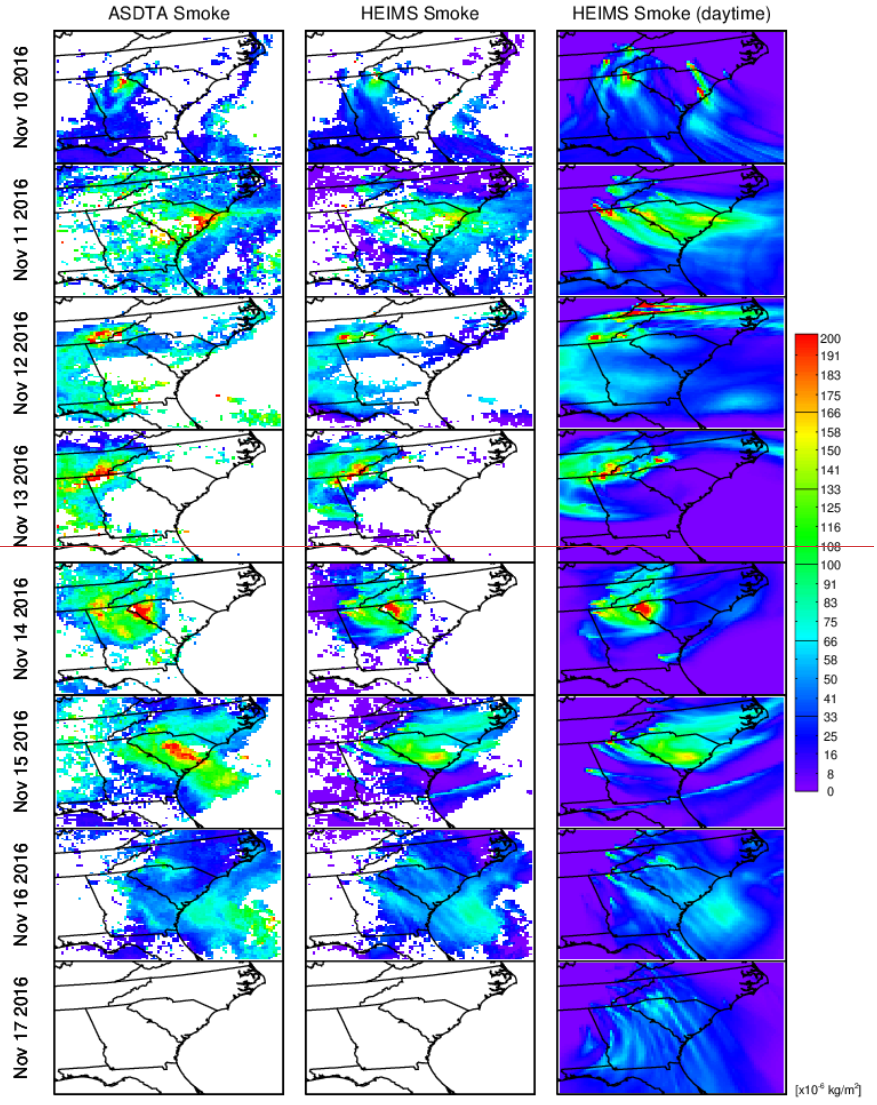
ASDTA Smoke
HEIMS Smoke
HEIMS Smoke (daytime)
Nov 10 2016
Nov 11 2016
Nov 12 2016
Nov 13 2016
Nov 14 2016
Nov 15 2016
Nov 16 2016
Nov 17 2016
200
191
183
175
166
158
150
141
133
125
116
108
100
91
83
75
66
58
50
41
33
25
16
8
0
[x10⁻⁶ kg/m³]

서식 있음: 가운데

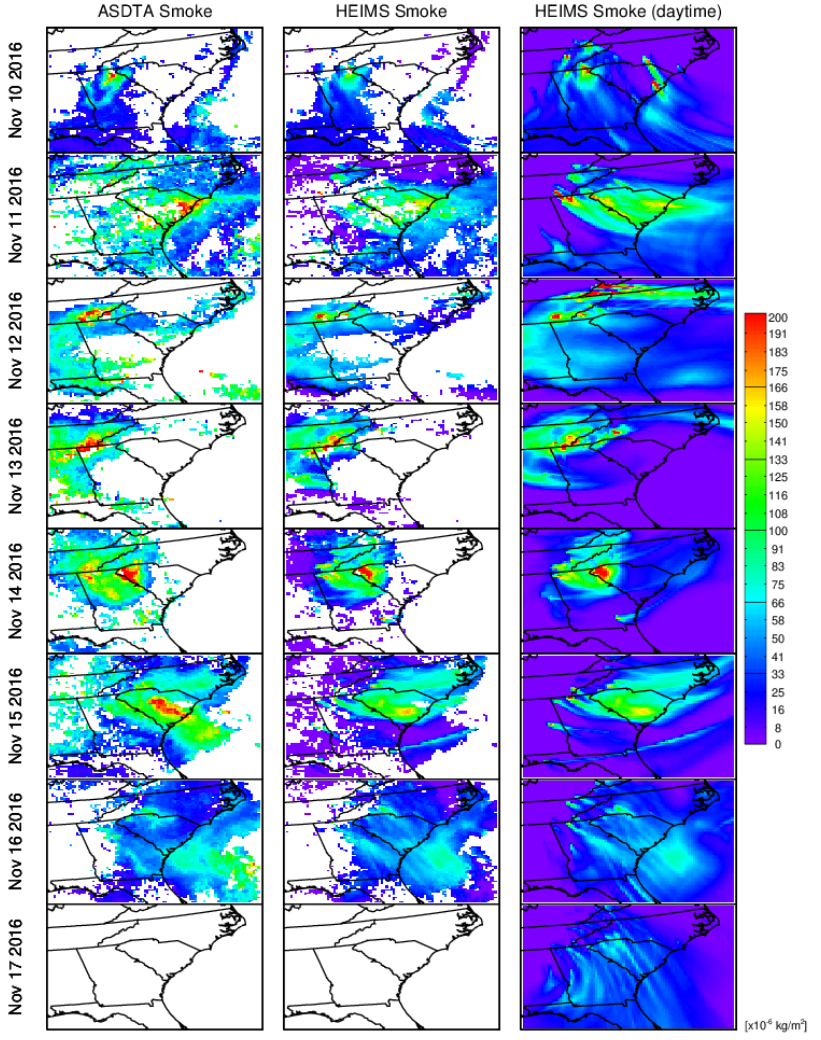
ASDTA Smoke
HEIMS Smoke
HEIMS Smoke (daytime)
Nov 10 2016
Nov 11 2016
Nov 12 2016
Nov 13 2016
Nov 14 2016
Nov 15 2016
Nov 16 2016
Nov 17 2016
200
191
183
175
166
158
150
141
133
125
116
108
100
91
83
75
66
58
50
41
33
25
16
8
0
[x10⁻⁶ kg/m³]

690

서식 있음: 가운데

Figure 5. Comparison of observed and reconstructed smoke plumes during November 10-17, 2016. Smoke mass loading from ASDTA (left) and reconstructed HEIMS smokes for ASDTA-matching (middle) and for daytime (right). A 48-hour observation (~~oday~~aday=-1) and 6-layer plume release configuration is used.

서식 지정함: 글꼴: 9 pt

서식 지정함: 글꼴: 9 pt

서식 있음: 간격 앞: 0 pt

서식 지정함: 글꼴: 9 pt

서식 있음: 가운데

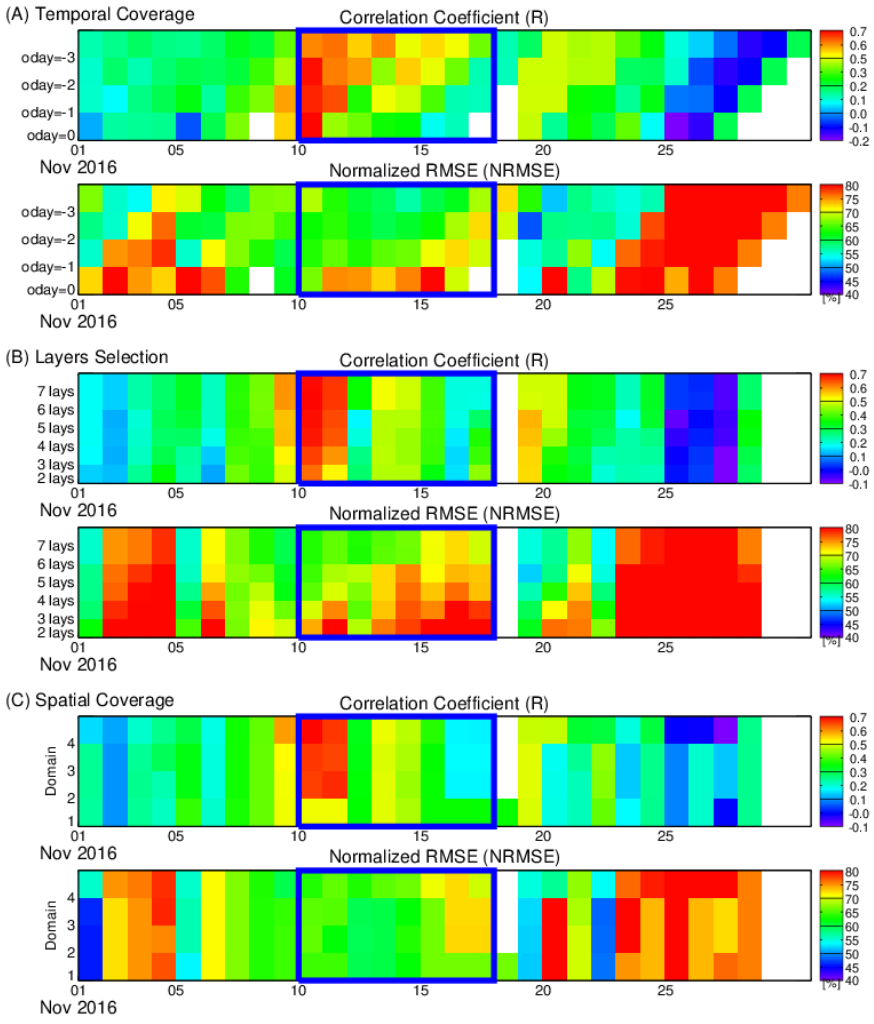

695

39

서식 있음: 가운데

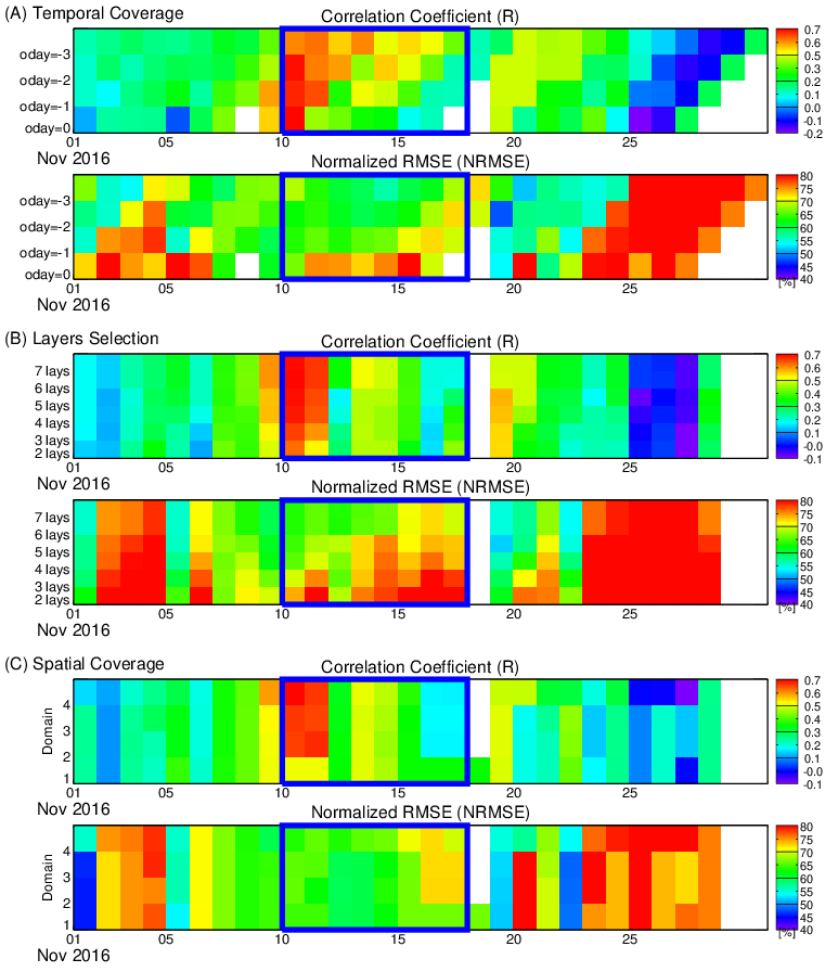

Figure 6. Sensitivity tests for (a) temporal coverage, (b) layer selection, and (c) spatial coverage. Temporal coverage of inputs is tested for between 24 hours (~~oday~~aday=0) and 96 hours (~~oday~~aday=-3). Selection of layers is tested using two to seven layers among 100, 500, 1000, 1500, 2000, 5000, and 10000 meters. Beginning from two layers at 100 and 500 meters, the next higher layer is added for each test. Spatial coverage is tested through domain 1 to 4. The thick blue boxes indicate the intensive fire episode period, November 10-17, 2016.

서식 지정함: 글꼴: 9 pt

서식 지정함: 글꼴: 9 pt

서식 지정함: 글꼴: 9 pt

서식 있음: 가운데

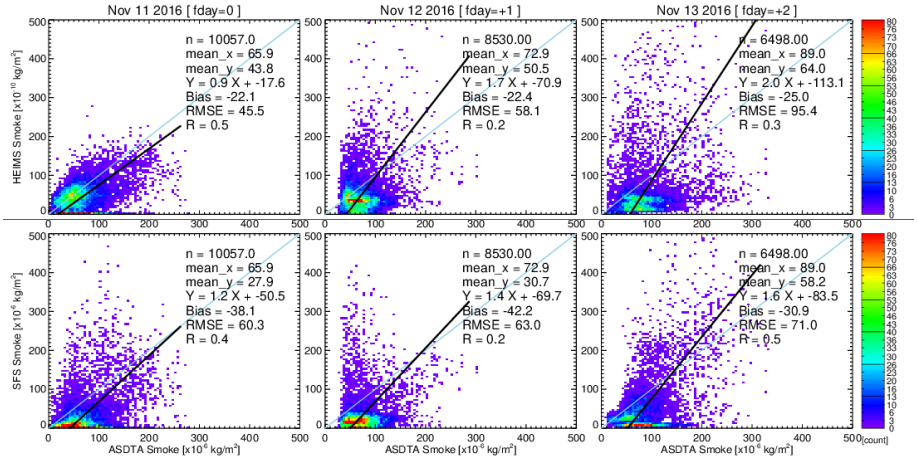
Nov 11 2016 [fday=0]
Nov 12 2016 [fday=+1]
Nov 13 2016 [fday=+2]
n = 10057.0
mean_x = 65.9
mean_y = 43.8
Y = 0.9 X + -17.6
Bias = -22.1
RMSE = 45.5
R = 0.5
n = 8530.00
mean_x = 72.9
mean_y = 50.5
Y = 1.7 X + -70.9
Bias = -22.4
RMSE = 58.1
R = 0.2
n = 6498.00
mean_x = 89.0
mean_y = 64.0
Y = 2.0 X + -113.1
Bias = -25.0
RMSE = 95.4
R = 0.3
HEIMS Smoke [x10^-10 kg/m^3]
n = 10057.0
mean_x = 65.9
mean_y = 27.9
Y = 1.2 X + -50.5
Bias = -38.1
RMSE = 60.3
R = 0.4
n = 8530.00
mean_x = 72.9
mean_y = 30.7
Y = 1.4 X + -69.7
Bias = -42.2
RMSE = 63.0
R = 0.2
n = 6498.00
mean_x = 89.0
mean_y = 58.2
Y = 1.6 X + -83.5
Bias = -30.9
RMSE = 71.0
R = 0.5
SFS Smoke [x10^-6 kg/m^3]
ASDTA Smoke [x10^-6 kg/m^2]
[count]

705

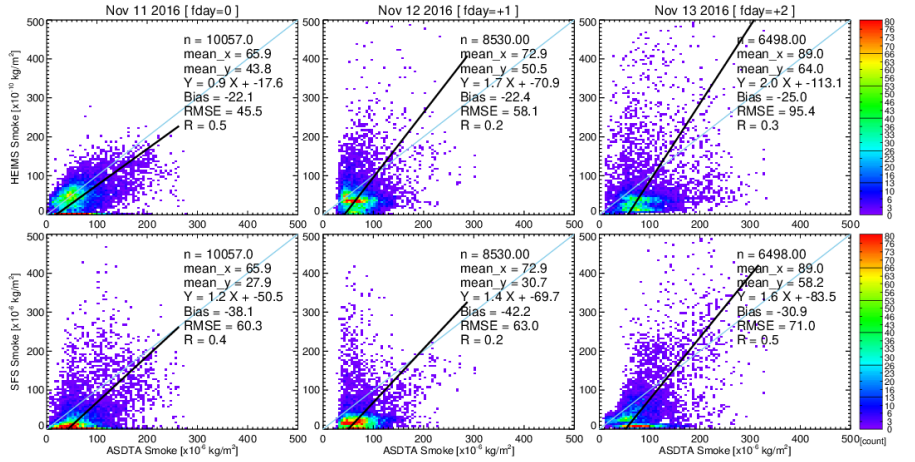
Nov 11 2016 [fday=0]
Nov 12 2016 [fday=+1]
Nov 13 2016 [fday=+2]
n = 10057.0
mean_x = 65.9
mean_y = 43.8
Y = 0.9 X + -17.6
Bias = -22.1
RMSE = 45.5
R = 0.5
n = 8530.00
mean_x = 72.9
mean_y = 50.5
Y = 1.7 X + -70.9
Bias = -22.4
RMSE = 58.1
R = 0.2
n = 6498.00
mean_x = 89.0
mean_y = 64.0
Y = 2.0 X + -113.1
Bias = -25.0
RMSE = 95.4
R = 0.3
HEIMS Smoke [x10^-10 kg/m^3]
n = 10057.0
mean_x = 65.9
mean_y = 27.9
Y = 1.2 X + -50.5
Bias = -38.1
RMSE = 60.3
R = 0.4
n = 8530.00
mean_x = 72.9
mean_y = 30.7
Y = 1.4 X + -69.7
Bias = -42.2
RMSE = 63.0
R = 0.2
n = 6498.00
mean_x = 89.0
mean_y = 58.2
Y = 1.6 X + -83.5
Bias = -30.9
RMSE = 71.0
R = 0.5
SFS Smoke [x10^-6 kg/m^3]
ASDTA Smoke [x10^-6 kg/m^2]
[count]

서식 있음: 가운데

Figure 7. Scatter plot comparisons between ASDTA smoke and HEIMS smoke (upper) and ASDTA and SFS smoke (lower) for forecast days, fday=0, +1, +2.

서식 지정함: 글꼴: 9 pt

서식 있음: 가운데

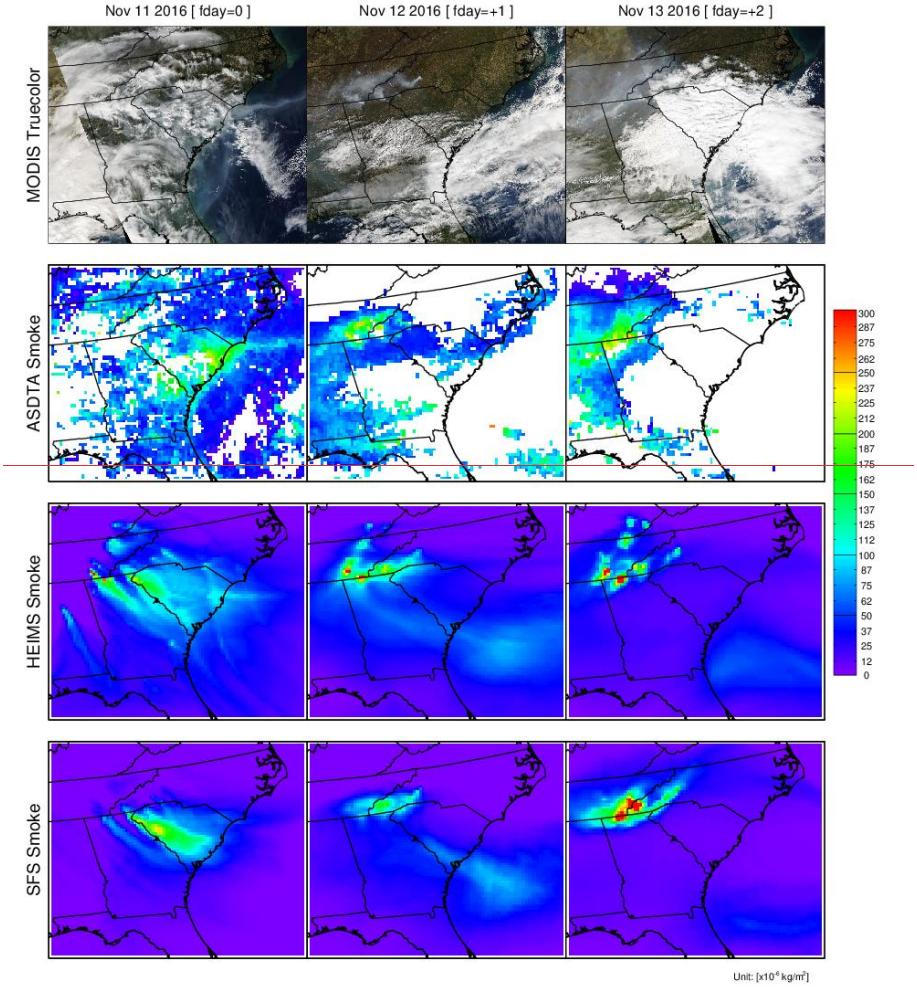
Nov 11 2016 [fday=0]
Nov 12 2016 [fday=+1]
Nov 13 2016 [fday=+2]
MODIS Truecolor
ASDTA Smoke
HEIMS Smoke
SFS Smoke
300
287
275
262
250
237
225
212
200
187
175
162
150
137
125
112
100
87
75
62
50
37
25
12
0
Unit: [x10⁻⁶ kg/m²]

서식 있음: 가운데

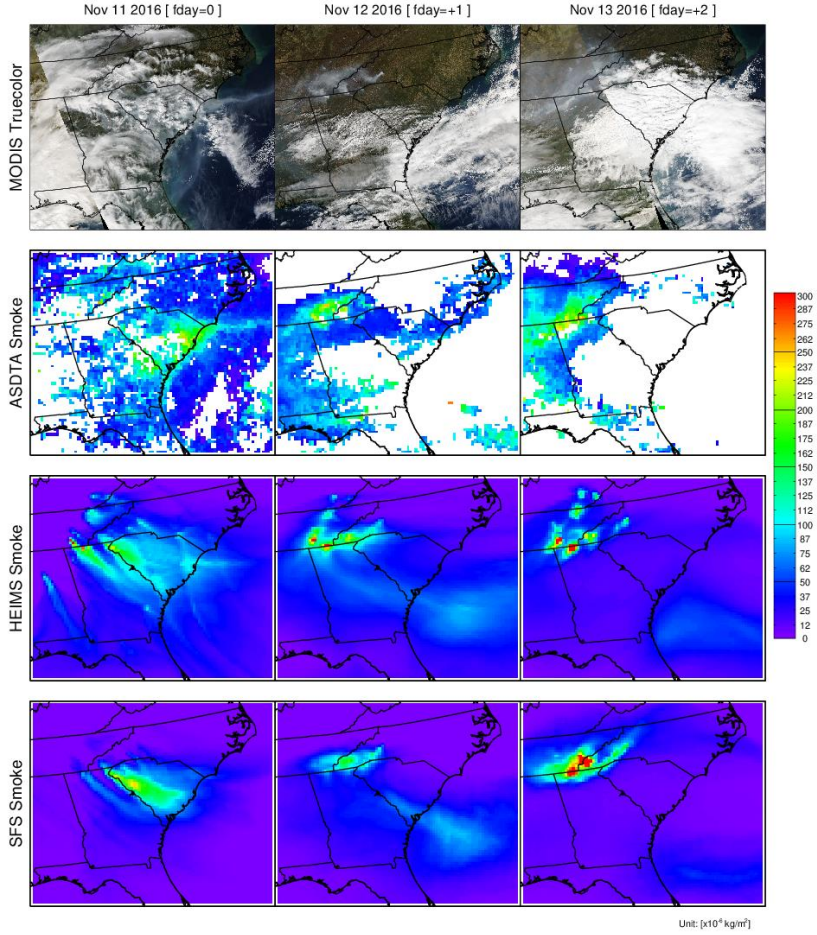

715 **Figure 8. Spatial distributions of observed and forecasted fire smoke plumes on November 11-13, 2016; Truecolor image from MODIS (1st row), ASDTA smoke (2nd row, converted from AOD), HEIMS smoke hindcast (3rd row), and SFS smoke forecast (4th row, from operation) are shown.**

서식 지정함: 글꼴: 9 pt

서식 있음: 가운데

서식 있음: 가운데

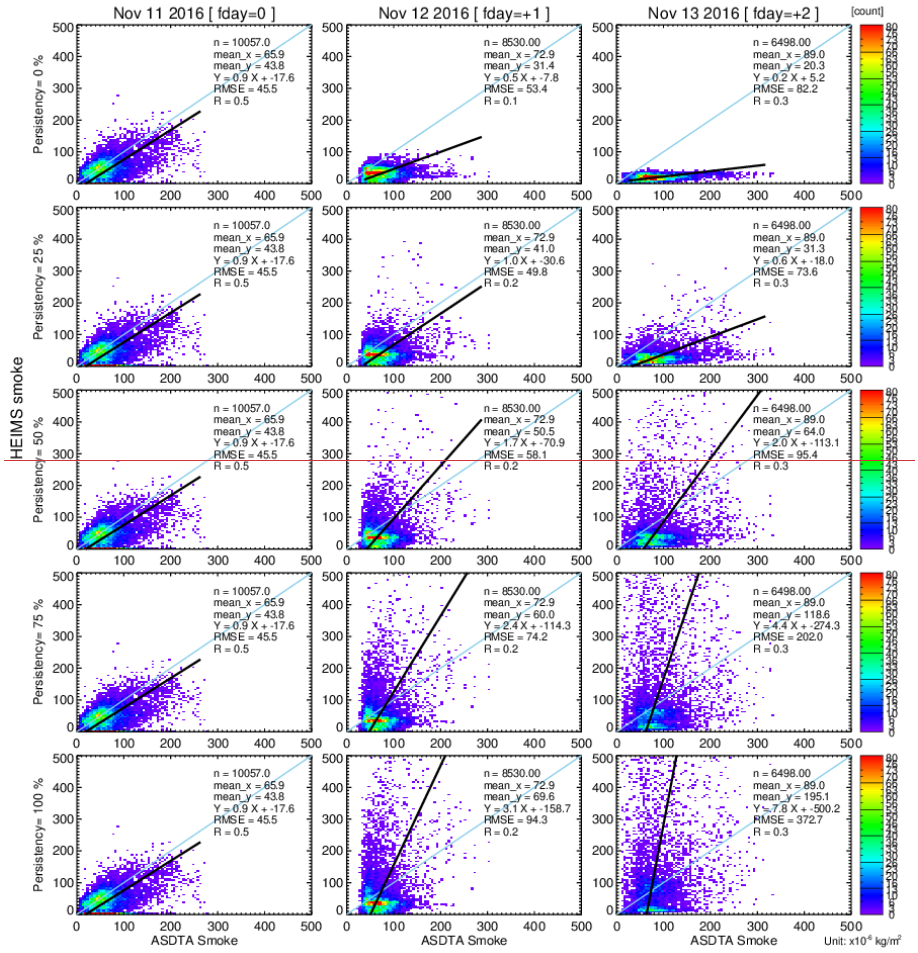
Nov 11 2016 [fday=0]
Nov 12 2016 [fday=+1]
Nov 13 2016 [fday=+2]
[count]
HEIMS smoke
Persistency= 0 %
Persistency= 25 %
Persistency= 50 %
Persistency= 75 %
Persistency= 100 %
n = 10057.0
mean_x = 65.9
mean_y = 43.8
Y = 0.9 X + -17.6
RMSE = 45.5
R = 0.5
n = 8530.00
mean_x = 72.9
mean_y = 31.4
Y = 0.5 X + -7.8
RMSE = 53.4
R = 0.1
n = 6498.00
mean_x = 89.0
mean_y = 20.3
Y = 0.2 X + 5.2
RMSE = 82.2
R = 0.3
mean_y = 41.0
Y = 1.0 X + -30.6
RMSE = 49.8
R = 0.2
mean_y = 31.3
Y = 0.6 X + -18.0
RMSE = 73.6
R = 0.3
mean_y = 50.5
Y = 1.7 X + -70.9
RMSE = 58.1
R = 0.2
mean_y = 64.0
Y = 2.0 X + -113.1
RMSE = 95.4
R = 0.3
mean_y = 60.0
Y = 2.4 X + -114.3
RMSE = 74.2
R = 0.2
mean_y = 118.6
Y = 4.4 X + -274.3
RMSE = 202.0
R = 0.3
mean_y = 69.6
Y = 3.1 X + -158.7
RMSE = 94.3
R = 0.2
mean_y = 195.1
Y = 7.8 X + -500.2
RMSE = 372.7
R = 0.3
ASDTA Smoke
Unit: x10^6 kg/m^2

720

서식 있음: 가운데

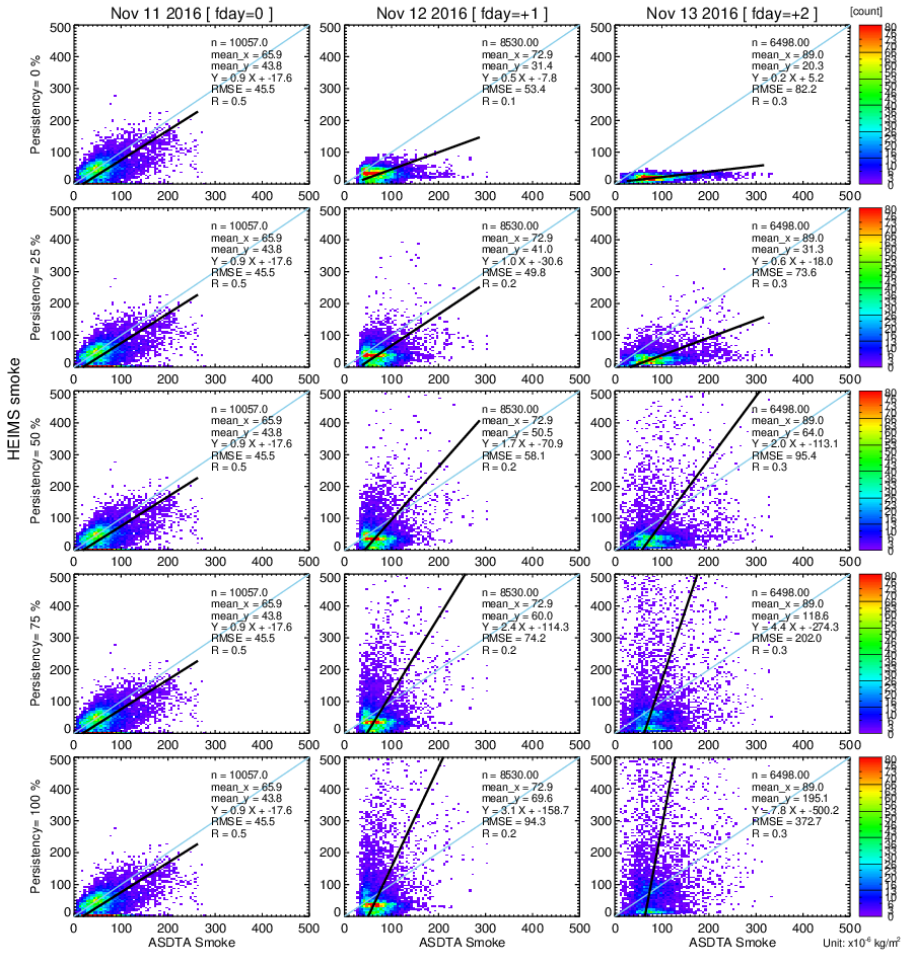

Figure 9. Sensitivity test with varying persistent rates. For p =75%, we assume 75% of fday=0 emissions last in fday=+1, and 75%^2 emissions last in fday=+2.

서식 지정함: 글꼴: 굵게 없음

서식 있음: 가운데

서식 있음: 캡션

서식 있음: 가운데